Short communication

Comparison of serum sensitivities of pseudotype retroviruses produced from newly established packaging cell lines of human and feline origins

Rie Watanabe[a], Takayuki Miyazawa[a,b,*,1], Yoshiharu Matsuura[a]

[a] Research Center for Emerging Infectious Diseases, Research Institute for Microbial Diseases, Osaka University, 3-1 Yamadaoka, Suita, Osaka 565-0872, Japan

[b] Host and Defence, PRESTO, Japan Science and Technology Agency, 4-1-8 Honcho Kawaguchi, Saitama 332-0012, Japan

Abstract

To apply retrovirus vectors for in vivo gene therapy in cats, it is necessary to develop vector systems that are not inactivated by cat serum. In this study, the retrovirus packaging cell lines 2SC-1 and AHCeB7 were newly established from human embryonic kidney (HEK) 293 and feline fibroblastic AH927 cells, respectively. Then the sensitivities of pseudotype viruses released from these cell lines to fresh sera from humans and cats were compared. Pseudotype viruses from the 2SC-1 cells were inactivated efficiently by cat serum but not by human serum. Pseudotype viruses from the AHCeB7 cells were also inactivated efficiently by human serum, however they were rather resistant to cat serum. When the xenoantigenicity of the cell lines was examined by flow cytometry, AH927 cells reacted with human serum, however, HEK293 cells did not react with cat serum. These results suggested that pseudotype viruses from 2SC-1 cells were inactivated by the fresh cat serum in an antibody-independent manner. Chelating experiments revealed that certain temperature-sensitive factor(s) other than complements might be involved in the inactivation. The usage of feline cells as packaging cells is suitable for in vivo gene therapy in cats.
© 2003 Elsevier B.V. All rights reserved.

Keywords: Cats; FeLV; Gene therapy; Packaging cells; Serum sensitivity

Viral vectors based on retroviruses, such as murine leukemia virus (MLV) and human immunodeficiency virus, are powerful tools for gene delivery in vitro and in vivo (for a review, see reference Takeuchi and Pizzato, 2000). For in vivo gene therapy, it is necessary to develop vectors resistant to serum. In terms of human in vivo gene therapy, there have been many reports on retrovirus vectors which can not be inactivated by human serum (Kafri, 2001; Quinonez and Sutton, 2002). However, retroviral vector systems effective for in vivo gene transfer in domestic cats have not been established so far.

Since retroviruses except spumaviruses bud from the cell membrane, they incorporate components expressed on the cell membrane into the virion membrane. Humans have natural antibodies against xenoantigens expressed on non-primate cells such as murine cells (Takeuchi et al., 1996, 1997). These natural antibodies can bind to the virion membrane and lyse retroviruses via activation of the classical complement pathway. Thus, human serum efficiently inactivates retroviruses produced from non-primate cells. Similar to humans, cats may have natural antibodies against xenoantigens expressed on non-feline mammalian cells, and cat serum may inactivate retrovirus particles. In addition to antibody-dependent inactivation, retroviral particles might be lysed by activation of an antibody-independent alternative or mannan-binding-lectin (MBL) complement pathway (Favoreel et al., 2003).

In this study, we newly established MLV-based packaging cell lines derived from human and feline cells. From these packaging cell lines, we generated cell lines producing pseudotype viruses which have the envelope of feline leukemia virus subgroup B (FeLV-B) and express a reporter gene. Then, we compared the sensitivities of the pseudotype

* Corresponding author. Tel.: +81-155-49-5392; fax: +81-155-49-5394.

E-mail address: takavet@mc.kcom.ne.jp (T. Miyazawa).

1 Present address: Department of Veterinary Public Health, Obihiro University of Agriculture and Veterinary Medicine, Inada-cho, Obihiro, Hokkaido 080-8555, Japan.
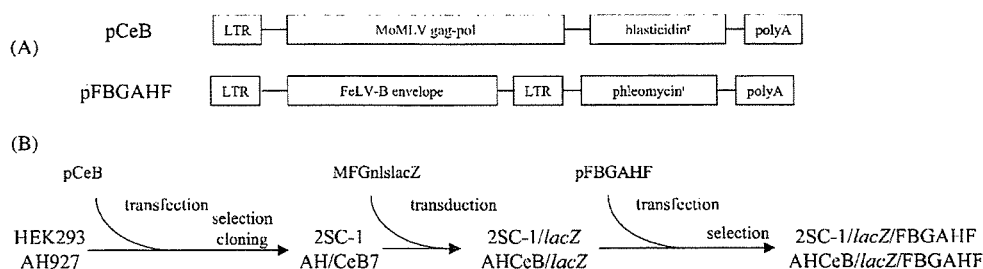
Fig. 1. Establishement of the pesudotype virus-producing cell lines. (A) Schematic representation of plasmid constructs used in this study. MoMLV *gag-pol* expression plasmid, pCeB and FeLV-B envelope expression plasmid, pFBFeLV-B are illustrated. Abbreviations: LTR, long terminal repeat; poly A, poly-adenylation signal. (B) Flow chart of procedures of establishment of pseudotype virus-producing cell lines.

viruses released from these cells to sera from humans and cats, and also examined the xenoantigenicity of the packaging cell lines by flow cytometry.

Human embryonic kidney (HEK) 293 cells, AH927 cells (feline fibroblast cell line), NIH3T3 cells (mouse fibroblast cell line) and TELCeB/SALF cells (Cosset et al., 1995) (a derivative of TE671 cells (human rhabdomyosarcoma cells) producing LacZ pseudotype viruses) were grown in Dulbecco's modified Eagle's medium (DMEM) (Sigma, St. Louis, MI, USA) supplemented with 10% fetal calf serum (FCS), penicillin (100 units/ml) and streptomycin (100 μg/ml).pCeB [1], an expression vector for the Moloney MLV (MoMLV) *gag-pol* gene as well as a blasticidin resistant selectable marker (Fig. 1A), was kindly provided by Dr. Y. Takeuchi (University College London, London, UK). The construction of an *env* expression plasmid for FeLV-B, termed pFBGAHF (Fig. 1A), was described previously (Nakata et al., 2003). pCAGVSV-G, an expression plasmid for the G protein of vesicular stomatitis virus (VSV), and pMX-EGFP, a vector plasmid to express enhanced green fluorescence protein (EGFP), were described elsewhere (Misawa et al., 2000; Matsuura et al., 2001).

For establishment of Gag-Pol producing HEK293 cells (Fig. 1B), HEK293 cells were seeded at a concentration of 4.0 × 10^5 cells per 35 mm plate the day before transfection. Then, 1 μg of pCeB was transfected using FuGene6 (Roche, Basel, Germany). Two days after transfection, the cells were transferred to two 100 mm plates (Greiner, Frickienhausen, Germany), and selected with 4 μg/ml of Blasticidin S (Calbiochem, Schwalbach, Germany). The selection medium was replaced every 3 days until resistant cell colonies had appeared. Two weeks after the selection, the resistant colonies were picked up using penicillin cups, and further grown in 12-well plates (Greiner) for the assessment of reverse transcriptase (RT) production.

For establishment of Gag-Pol producing AH927 cells (Fig. 1B), AH927 cells were seeded in a 25 cm^2 flask the day before transfection. Then, 10 μg of pCeB was transfected by the calcium phosphate coprecipitation method (Graham and van der Eb, 1973). Four hours after transfection, the cells were washed twice with FCS-free medium and glycerol-shocked, and then the culture medium was replaced with fresh medium. Two days after transfection, the cells were transferred to two 75 cm^2 flasks and selected with 4 μg/ml of Blasticidin S. The resistant cells were cloned by the limiting dilution method using conditioned medium. Each cell clone was expanded in 25 cm^2 flasks for the assessment of RT activity.

Mn^{2+}-dependent RT activity in the culture supernatants from blasticidin-resistant 293 clones was measured using a Reverse Transcriptase Assay, Chemiluminescent (Roche) following the manufacturer's instructions using MnCl$_2$ instead of MgCl$_2$. The Mn^{2+}-dependent RT activity in the cell culture supernatants of blasticidin-resistant AH927 clones was assayed using [α-^{32}P]dTTP as described previously (Ohki et al., 1992). Briefly, 10 μl of the culture supernatant was mixed with a reaction mixture containing poly(rA)-oligo(dT) and [α-^{32}P]dTTP. After incubation for 3 h at 37 °C, the mixture was dotted on DEAE filter paper (DE81) (Whatmann, Kent, UK). RT activity was measured using scintillation.

The Gag-Pol expressing cell clones were introduced with a vector plasmid MFGnlsLacZ (Ferry et al., 1991) that expresses the *lacZ* gene with a nuclear localization signal. Cells were seeded at a concentration of 1 × 10^4 cells per well of six-well plates and inoculated with a helper-free MFGnlslacZ pseudotype virus bearing an envelope of amphotropic MLV (MLV-A) in the presence of 8 μg/ml of polybrene. The MFGnlslacZ pseudotype viruses were prepared from the culture supernatant of TELCeB/SALF cells as described previously (Cosset et al., 1995). Two days after infection, some of the cells were stained with 5-bromo-4-chloro-3-indolyl β-D-galactopyranoside (X-gal) (Sigma) as described previously (Sanes et al., 1986). Infection with the MFGnlslacZ pseudotype viruses and X-gal staining were repeated until more than 95% of the infected cells became *lacZ*-positive.

The *lacZ*-positive cell clones were seeded at a concentration of 4 × 10^5 cells per 35 mm plate (Greiner) the day before transfection. Then, 1 μg of pFBGAHF was transfected using FuGene6. Two days after transfection, the cells were transferred into 75 cm^2 flasks (Corning, NY, USA) and selected with 50 μg/ml of phleomycin (Sigma). Two weeks after selection, phleomycin resistant cell populations were obtained. The culture supernatants were harvested from the

confluent cell cultures in the presence or absence of FCS, filtrated through a 0.45 μm filter (Millipore, Bedfold, MA, USA), and used immediately for the infection assays.

For titration of LacZ pseudotype virus, target cells were seeded at a concentration of 3 × 10⁴ cells for both AH927 and NIH3T3, and 5 × 10⁴ cells for HEK293 in 0.25 ml per well of 48-well plates the day before infection. Cells were inoculated with 100 μl of serially diluted viruses in the presence of 8 μg/ml of polybrene. Four hours after infection, the virus was removed and the cells were cultured in the DMEM. Two days after infection, cells were stained with X-gal, and lacZ-positive foci were counted as described previously (Takeuchi et al., 1994).

From HEK293 cells transfected with pCeB (293/CeB), 34 blasticidin-resistant clones were obtained. Each clone was tested for the production of RT in the culture supernatants. Nine clones showed relatively high levels of RT activity (Fig. 2A). For titration of EGFP pseudotype virus, HEK293 cell clones expressing MLV Gag-Pol proteins were seeded at a concentration of 4 × 10⁵ cells per well of six-well plates the day before transfection. Then, 1 μg of pCAG-VSVG and 1 μg of pMX-EGFP were cotransfected using FuGene6. Two days after transfection, the culture medium was replaced with fresh medium. Then the culture supernatants were harvested after incubation overnight, filtrated through a 0.45 μm filter and used for the infection assay as described previously (Takeuchi et al., 1994). In brief, target HEK293 cells were seeded at a density of 2 × 10⁵ cells per well of 24-well plates the day before infection. Cells were inoculated with 500 μl of the serially diluted viruses in the presence of 8 μg/ml of polybrene. Four hours after infection, the inocula were removed and the cells were cultured in fresh medium. Two days after infection, EGFP-positive foci were counted.

After the transfection of pMX-EGFP and pCAG-VSVG into the clones, all clones produced EGFP pseudotype viruses bearing an envelope of VSV G proteins ranging from 1.5 × 10⁵ to 3.0 × 10⁶ focus forming units (ffu)/ml (Fig. 2B). Among the clones, we selected number 1 (designated 2SC-1) which showed the highest production of pseudotype viruses for further study.

From AH927 cells transfected with pCeB (AH/CeB), 24 blasticidin-resistant clones were obtained by the limiting dilution method. Because of the low transfection efficiency of the cells, AH/CeB clones were assessed only by RT production. Among the blasticidin-resistant clones, 10 showed relatively high levels of RT activity (Fig. 2A). Among these clones, we selected number 7 (designated AHCeB7) which showed the strongest RT activity for further study.

The 2SC-1 and AHCeB7 cells were introduced with a lacZ vector by infection. After confirming that more than 95% of the cells express the lacZ gene by X-gal staining, these cell lines were further transfected with pFB-GAHF and selected using phleomycin. Consequently, we obtained cell lines, designated 2SC-1/lacZ/FBGAHF and AHCeB/lacZ/FBGAHF, respectively, which produce LacZ pseudotype viruses. LacZ pseudotype viruses produced from 2SC-1/lacZ/FBGAHF and AHCeB/lacZ/FBGAHF were referred to as FeLV-B(lacZ)/2SC and FeLV-B(lacZ)/AH, respectively and were tested for transduction of the lacZ gene to HEK293, AH927 and NIH3T3 cells. These stable transfectants produced LacZ pseudotype viruses which can infect HEK293 and AH927 cells but not NIH3T3 cells. The titers of the pseudotype viruses were more than 10³ ffu/ml even in the absence of FCS during virus preparation and infection (Table 1). Pseudotype viruses prepared in the absence of FCS were subjected to serum sensitivity tests.
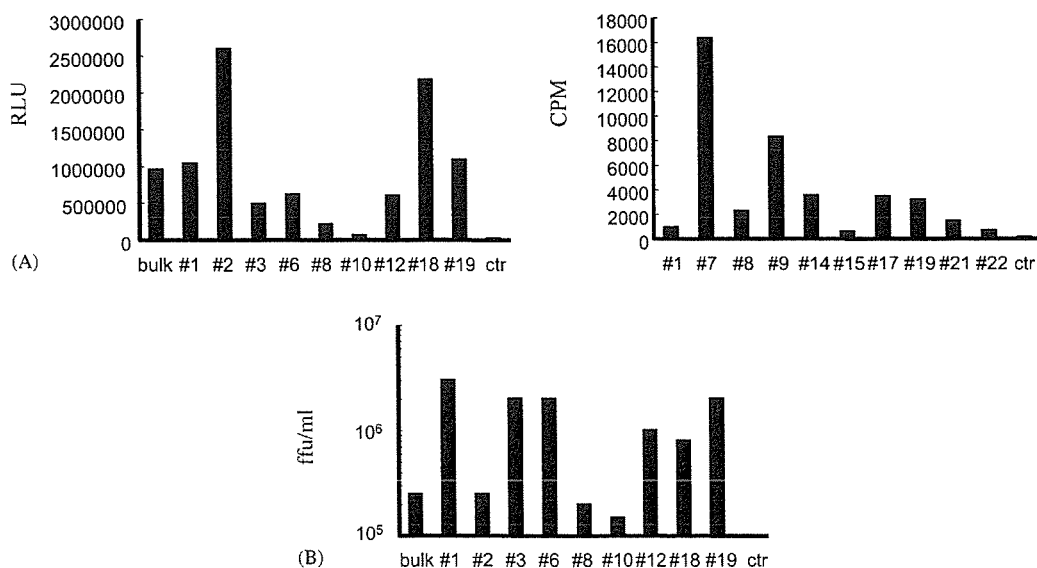

Fig. 2. (A) RT activities in the culture supernatants from 293/CeB (left) and AH927/CeB (right). RT activities are shown as the intensity of relative lights units (RLU) and counts per minute (CPM) of [α-³²P], respectively. (B) Infectious virus titers of EGFP-VSV G pseudotype viruses released from 293/CeB clones. EGFP-positive focus forming units (ffu) are shown.

Table 1
Titers of pseodotype viruses from producer cell lines in the absence of FCS

Target cells	Producer cell lines	
	2SC-1/lacZ/FBFeLV-B	AHCeB/lacZ/FBFeLV-B
HEK293	1.5×10^{4a}	1.0×10^4
AH927	3.0×10^3	3.5×10^3
NIH3T3	<10	<10

[a] Averages of titers (ffu/ml) of lacZ pseudotype viruses in three independent experiments are shown.

The sensitivity of lacZ pseudotype viruses to sera from humans and cats was examined by titrating the surviving viruses after incubation with 10% serum. In brief, the culture medium of each producer cell line was changed with FCS-free DMEM the day before the assay, and the culture supernatants were harvested. The harvested pseudotype viruses were incubated with fresh human or cat serum for 1 h at 37 °C. After incubation, the viruses were serially diluted and inoculated to target cells in the presence of 8 μg/ml of polybrene. Four hours after inoculation, the culture medium was replaced with fresh medium and the cells were incubated for an additional 2 days before X-gal staining. Since we found that HEK293 and AH927 cells were sensitive to lysis by fresh sera from cats and humans, respectively (data not shown), we used homologous target cells for the serum sensitivity test (i.e. HEK293 for the human serum and AH927 for the cat serum). FeLV-B(lacZ)/2SC was resistant to human serum but efficiently inactivated by cat serum (Table 2). In contrast, FeLV-B(lacZ)/AH was efficiently inactivated by human serum, however the viruses were relatively resistant to cat serum (Table 2). Heat-inactivated human and cat sera did not inactivate the pseudotype viruses at all (data not shown).

Finally, the xenoantigenicity of the cell lines was examined by flow cytometric analyses. Cells were harvested after 0.05% EDTA treatment for 10 min at 37 °C. After being washed with phosphate-buffered saline (PBS), the cells were reacted with 10% heat-inactivated cat or human

Table 2
Sensitivity of viruses for human and feline serum

Pseudotype virus	Target	Serum	Titer (ffu/ml)[a]	Percentage of reduction
FeLV-B(lacZ)/2SC	HEK 293	Control[b]	800	
		Human	800	0
	AH927	Control	1500	
		Cat	366	76
FeLV-B(lacZ)/AH	HEK293	Control	2500	
		Human	<10	100
	AH927	Control	7500	
		Cat	5030	33

[a] Averages of titers of lacZ pseudotype viruses in three independent experiments are shown.
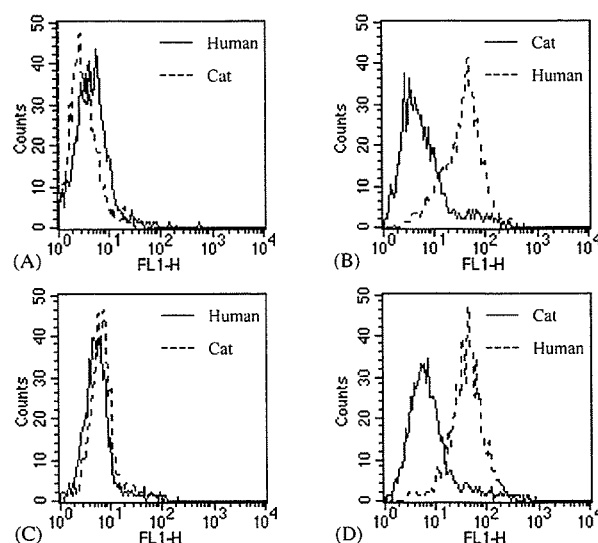[b] Pseudotype viruses were reacted with serum-free DMEM.

Fig. 3. Xenoantigenicity of HEK293, AH927 and their derivatives. HEK293 (A) and 2SC-1/lacZ/pFBGAHF cells (B) were reacted with heat-inactivated sera from humans (bold line) and cats (dotted line). AH927 (C) and AHCeB/lacZ/pFBGAHF cells (D) were reacted with heat-inactivated sera from cats (bold line) and humans (dotted line).

serum in serum-free DMEM on ice for 40 min. The cells were washed with PBS, and then reacted with fluorescein isothiocyanate-labeled anti-human whole immunoglobulin (Ig) (Molecular Probe, Eugene, OR, USA) or anti-feline whole Ig (ICN Biomedical, Aurora, OH, USA) at a final concentration of 0.002 μg/ml on ice for 40 min. After being washed with PBS, the cells were resuspended in 500 μl of PBS, and analyzed using a FACSCalibur (Becton Dickinson, San Jose, CA, USA). The data were analyzed using CellQuest software (Becton Dickinson). Human HEK293 cells did not react with sera from humans or cats (Fig. 3A). Feline AH927 cells reacted strongly with human serum but weakly with cat serum (Fig. 3C). The reactivity to the sera was not affected by the expression of MLV Gag-Pol and FeLV-B Env proteins in the cells (Fig. 3B and D).

In this study, we newly established two retrovirus packaging cell lines, AHCeB7 and 2SC-1, from feline AH927 and human HEK293 cells, respectively. After the introduction of a lacZ vector and FeLV-B Env expression plasmid, these cells produced LacZ pseudotype viruses. Using these pseudotype viruses, we compared the sensitivities of the viruses to fresh sera from humans and cats, and found that usage of feline cells as packaging cells is suitable for in vivo gene therapy in cats.

The most important difference at the cell surface between humans and other mammals except apes and old world monkeys is the existence of Gal(α1-3)Gal terminal carbohydrates ((α1-3)Gal) (Galili et al., 1985, 1987). Since humans and old world monkeys lack a functional (α1-3)galactosyltransferase (Larsen et al., 1990; Galili and Swanson, 1991), they have no (α1-3)Gal terminal structure and develop abundant anti-(α1-3)Gal antibodies in their sera

(Galili et al., 1985). Virions released from nonprimate cells incorporate the (α1-3)Gal (Takeuchi et al., 1996, 1997). Retroviruses bearing the (α1-3)Gal epitope are immediately inactivated by human serum (Rother et al., 1995).

Here, we also confirmed that human serum efficiently inactivated the pseudotype viruses from feline AH927 cells but not those from human HEK293 cells. On the other hand, cat serum efficiently inactivated the pseudotype viruses from HEK293 cells. Since cat serum did not react with 2SC-1/*lacZ*/FBGAHF cells in the flow cytometric analyses (Fig. 3) and heat-inactivated cat sera did not inactivate the pseudotype viruses, we considered that most of the pseudotype viruses have been inactivated by complement in an Ab-independent manner, i.e. alternative or MBP complement pathway. To determine which pathway is involved in the neutralization, the effects of depletion of Ca^{2+} and Mg^{2+} were examined. Ca^{2+} is essential for the classical and MBL complement pathways, whereas the alternative pathway can be activated in the presence of Mg^{2+} instead of Ca^{2+}. Contrary to our expectation, no effects were observed when both Ca^{2+} and Mg^{2+} or Ca^{2+} alone were chelated by 10 mM EDTA or EGTA, respectively (data not shown). These results suggested that certain temperature-sensitive factor(s) other than complements might be involved in this neutralization although the nature of the factor(s) is still unknown at present.

Acknowledgements

References

Cosset, F.L., Takeuchi, Y., Battini, J.L., Weiss, R.A., Collins, M.K., 1995. High-titer packaging cells producing recombinant retroviruses resistant to human serum. J. Virol. 69, 7430–7436.

Favoreel, H.W., Van de Walle, G.R., Nauwynck, H.J., Pensaert, M.B., 2003. Virus complement evasion stategies. J. Gen. Virol. 84, 1–15.

Ferry, N., Duplessis, O., Houssin, D., Danos, O., Heard, J.M., 1991. Retroviral-mediated gene transfer into hepatocytes in vivo. Proc. Natl. Acad. Sci. U.S.A. 88, 8377–8381.

Galili, U., Swanson, K., 1991. Gene sequences suggest inactivation of alpha-1,3-galactosyltransferase in catarrhines after the divergence

of apes from monkeys. Proc. Natl. Acad. Sci. U.S.A. 88, 7401–7404.

Galili, U., Macher, B.A., Buehler, J., Shohet, S.B., 1985. Human natural anti-alpha-galactosyl IgG. II. The specific recognition of alpha (1,3)-linked galactose residues. J. Exp. Med. 162, 573–582.

Galili, U., Clark, M.R., Shohet, S.B., Buehler, J., Macher, B.A., 1987. Evolutionary relationship between the natural anti-Gal antibody and the Gal alpha 1-3Gal epitope in primates. Proc. Natl. Acad. Sci. U.S.A. 84, 1369–1373.

Graham, F.L., van der Eb, A.J., 1973. A new technique for the assay of infectivity of human adenovirus 5 DNA. Virology 52, 456–467.

Kafri, T., 2001. Lentivirus vectors: difficulties and hopes before clinical trials. Curr. Opin. Mol. Ther. 3, 316–326.

Larsen, R.D., Rivera-Marrero, C.A., Ernst, L.K., Cummings, R.D., Lowe, J.B., 1990. Frameshift and nonsense mutations in a human genomic sequence homologous to a murine UDP-Gal: beta-D-Gal (1, 4)-D-GlcNAc alpha (1,3)-galactosyltransferase cDNA. J. Biol. Chem. 265, 7055–7061.

Matsuura, Y., Tani, H., Suzuki, K., Kimura-Someya, T., Suzuki, R., Aizaki, H., Ishii, K., Moriishi, K., Robison, C.S., Whitt, M.A., Miyamura, T., 2001. Characterization of pseudotype VSV possessing HCV envelope proteins. Virology 286, 263–275.

Misawa, K., Nosaka, T., Morita, S., Kaneko, A., Nakahata, T., Asano, S., Kitamura, T., 2000. A method to identify cDNAs based on localization of green fluorescent protein fusion products. Proc. Natl. Acad. Sci. U.S.A. 97, 3062–3066.

Nakata, R., Miyazawa, T., Shin, Y.-S., Watanabe, R., Mikami, T., Matsuura, Y., 2003. Reevaluation of host ranges of feline leukemia virus subgroups. Microbes Infect. 5, 947–950.

Ohki, K., Kishi, M., Ohmura, K., Morikawa, Y., Jones, I.M., Azuma, I., Ikuta, K., 1992. Human immunodeficiency virus type 1 (HIV-1) superinfection of a cell clone converting it from production of defective to infectious HIV-1 is mediated predominantly by CD4 regions other than the major binding site for HIV-1 glycoproteins. J. Gen. Virol. 73, 1761–1772.

Quinonez, R., Sutton, R.E., 2002. Lentiviral vectors for gene delivery into cells. DNA Cell. Biol. 21, 937–951.

Rother, R.P., Fodor, W.L., Springhorn, J.P., Birks, C.W., Setter, E., Sandrin, M.S., Squinto, S.P., Rollins, S.A., 1995. A novel mechanism of retrovirus inactivation in human serum mediated by anti-alpha-galactosyl natural antibody. J. Exp. Med. 182, 1345–1355.

Sanes, J.R., Rubenstein, J.L., Nicolas, J.F., 1986. Use of a recombinant retrovirus to study postimplantation cell linage in mouse embryos. EMBO J. 5, 3133–3142.

Takeuchi, Y., Pizzato, M., 2000. Retrovirus vectors. Adv. Exp. Med. Biol. 465, 23–35.

Takeuchi, Y., Cosset, F.L., Lachmann, P.J., Okada, H., Weiss, R.A., Collins, M.K., 1994. Type C retrovirus inactivation by human complement is determined by both the viral genome and the producer cell. J. Virol. 68, 8001–8007.

Takeuchi, Y., Liong, S.H., Bieniasz, P.D., Jager, U., Porter, C.D., Friedman, T., McClure, M.O., Weiss, R.A., 1997. Sensitization of rhabdo-, lenti-, and spumaviruses to human serum by galactosyl(α1-3)galactosylation. J. Virol. 71, 6174–6178.

Takeuchi, Y., Porter, C.D., Strahan, K.M., Preece, A.F., Gustafsson, K., Cosset, F.L., Weiss, R.A., Collins, M.K., 1996. Sensitization of cells and retroviruses to human serum by (α1-3) galactosyltransferase. Nature 379, 85–88.

ELSEVIER

Evidence for a polytopic form of the E1 envelope glycoprotein of Hepatitis C virus

Christopher T. Migliaccio [a], Kathryn E. Follis [a], Yoshiharu Matsuura [b], Jack H. Nunberg [a],*

[a] *Science Complex Room 221, Montana Biotechnology Center, The University of Montana, Missoula, MT 59812, USA*
[b] *Research Center for Emerging Infectious Diseases, Research Institute for Microbial Diseases, Osaka University, Osaka 565-0871, Japan*

Abstract

The polyprotein precursor of the Hepatitis C virus (HCV) contains multiple membrane-spanning domains that define the membrane topology and subsequent maturation of the viral structural proteins. In order to examine the biogenesis of the E1–E2 heterodimeric complex, we inserted an affinity tag (S-peptide) at specific locations within the envelope glycoproteins. In particular, and based on the prediction that the E1 glycoprotein may be able to assume a polytopic topology containing two membrane-spanning domains, we inserted the affinity tag within a putative cytoplasmic loop of the E1 glycoprotein. The HCV structural polyprotein containing this tag (at amino acids 295/296) was highly expressed and able to form a properly processed and noncovalently associated E1–E2 complex. This complex was bound by murine and conformation-dependent human monoclonal antibodies (MAbs) comparably to the native untagged complex. In addition, MAb recognition was retained upon reconstituting the tagged E1–E2 complex in lipid membrane as topologically constrained proteoliposomes. Our findings are consistent with the model of a topologically flexible E1 glycoprotein that is able to adopt a polytopic form. This form of the E1–E2 complex may be important in the HCV life cycle and in pathogenesis.
© 2004 Elsevier B.V. All rights reserved.

Keywords: Hepatitis C virus; Envelope glycoprotein; E1–E2 complex; Membrane topology; Affinity tag; Proteoliposome

1. Introduction

Hepatitis C virus (HCV) is a major cause of chronic hepatitis and liver cirrhosis worldwide. It is estimated that over 170 million persons are infected with HCV and at risk for hepatocellular carcinoma (World Health Organization, 1999). HCV is an enveloped RNA virus and the sole member of the *Hepacivirus* genus within the Flaviviridae family. The single-stranded, positive-sense RNA genome of HCV contains a single open-reading frame that encodes a viral polyprotein precursor of approximately 3000 amino acids (Grakoui et al., 1993; Selby et al., 1993). Membrane-spanning domains within the polyprotein force threadings through the membrane of the rough endoplasmic reticulum (ER) and the mature viral proteins are liberated from the precursor polyprotein by the action of viral and cellular proteases ((Dubuisson, 2000; Reed and Rice, 2000)

and references therein). The structural proteins of the virus are contained in the N-terminal portion of the polyprotein (in order: Core and the E1 and E2 envelope glycoproteins) and are generated by signal peptidase cleavage in the lumen of the ER. A small membrane protein of unknown function, p7, is encoded downstream of the E2 glycoprotein and is also produced by cellular signal peptidase. The nonstructural proteins of the virus (NS2, NS3, NS4A and B and NS5A and B) are contained in the C-terminal portion of the polyprotein and lie on the cytosolic side of the ER membrane. The mature NS proteins are generated by viral proteases in the cytoplasm. Because there is no robust cell culture system for HCV propagation (reviewed by (Bartenschlager and Lohmann, 2001)), details of envelope glycoprotein biogenesis and virion assembly have not been studied under conditions of productive infection.

Multiple membrane-spanning domains define the topology of the HCV polyprotein precursor during biogenesis. Biochemical and genetic studies indicate that the E1 and E2 glycoproteins adopt a Type I (von Heijne, 1988) topol-

ogy in the ER membrane: each glycoprotein is anchored by a single C-terminal transmembrane domain and presents an N-terminal ectodomain ((Op De Beeck et al., 2001) and references therein). The C-terminal membrane-spanning domains of the HCV E1 and E2 glycoproteins also encode the signal peptide sequences of the downstream proteins (E2 and p7, respectively); the signal peptide of the E1 glycoprotein is contained within the C-terminal region of Core. These transmembrane domains are additionally important for the formation of the properly folded, noncovalently associated E1–E2 complex (Michalak et al., 1997; Op De Beeck et al., 2000; Patel et al., 2001). During biosynthesis, the HCV envelope glycoproteins are slow to fold properly (Choukhi et al., 1998; Dubuisson and Rice, 1996; Merola et al., 2001), and misfolding is thought to result in the isolation of predominantly disulfide-crosslinked complexes. In addition, the transmembrane domains also function as ER retention signals that largely prevent progress of the E1–E2 complex through the exocytic pathway (Cocquerel et al., 1998; Cocquerel et al., 1999; Dubuisson et al., 1994; Duvet et al., 1998; Flint and McKeating, 1999). Recent studies indicate that some E1–E2 complex may be transported to the plasma membrane (Bartosch et al., 2003; Drummer et al., 2003; Hsu et al., 2003).

In order to study the biogenesis of the HCV envelope glycoproteins, we have defined conditions for the isolation of noncovalently associated E1–E2 complexes. To probe this structure, we have introduced an affinity tag at specific locations in E1, E2 and p7. Here, we show that the E1 glycoprotein can readily accommodate a tag at position 295/296 — in a region bounded by a predicted transmembrane helix on one side and the C-terminal transmembrane domain on the other. Affinity purification and membrane reconstitution of the tagged E1–E2 complex suggests that the E1 glycoprotein may exhibit topologic flexibility that includes a polytopic form in which the tagged region comprises a cytoplasmic loop joining two membrane-spanning regions. The existence of a topologically distinct form of the E1–E2 complex may have important implications in HCV biology and pathogenesis.

2. Materials and methods

2.1. HCV expression plasmids

The infectious HCV cDNA (genotype 1b) used in these studies was originally isolated from an HCV carrier (Aizaki et al., 1998) and the region encoding Core, the E1 and E2 glycoproteins and p7 was adapted to enable translation of the structural portion of the polyprotein (pCAG HCV aa 1–810, (Takikawa et al., 2000)). The numbering of the HCV amino acids is from the initiating methionine of the polyprotein. The pCAG HCV expression cassette (BglII–BglII) was transferred to the BamHI site of pcDNA 3.1 (Invitrogen) and a properly oriented insert was identified. The unique KpnI

site within the pcDNA 3.1 polylinker was subsequently destroyed in pHCV–ΔKpn to facilitate subsequent manipulations.

The PHD-htm algorithm (Rost et al., 1995); accessed at (Columbia University Bioinformatics Center, 2002) was used to predict transmembrane helical regions within the HCV structural proteins. Based on these predictions and other considerations described in the text, sites of potential cytosolic exposure in E1, E2 and p7 were identified and engineered to include the 15 amino acid S-peptide (Spep) affinity tag KETAAAKFERQHMDS (Kim and Raines, 1993; Fig. 1A).

Molecular cloning to insert a DNA sequence encoding the affinity tag within the HCV membrane proteins utilized two oligonucleotides. The upstream oligonucleotide included, at its 3' end, a sequence complementary to that encoding HCV amino acids N-terminal to the Spep insertion site. This was followed (in the 5' direction on the oligonucleotide primer) by a sequence complementary to that encoding a triple glycine (Gly₃) linker, the Spep, and another Gly₃ linker. The latter Gly₃ was followed by an additional threonine that enabled the inclusion of a KpnI site (GGT ACC) near the 5' end of the oligonucleotide. The second primer was complementary to the KpnI site and included at its 3' end a sequence encoding HCV amino acids C-terminal to the Spep insertion site. Using the pHCV–ΔKpn plasmid, these two oligonucleotides were extended for 25 cycles of PCR using Herculase DNA Polymerase (Stratagene). Following DpnI digestion to inactivate the original plasmid, the mixture was digested with KpnI and the newly synthesized plasmid was allowed to recircularize in the presence of T4 DNA ligase. Transformation of Escherichia coli resulted in the recovery of plasmids encoding a perfect splice of the Gly₃-Spep-Gly₃-Thr cassette within the respective E1, E2 and p7 coding regions. The insertions were confirmed by DNA sequencing. Three clones of each were carried forward in subsequent expression studies to exclude the possibility of adventitious changes elsewhere. The resulting plasmids encoding Spep-tagged HCV Core-E1-E2-p7 polyprotein are identified as E1Spep, E2Spep and p7Spep, respectively. For some studies, p7 expression was ablated from the HCV and E1Spep constructs by the introduction of a TAA stop codon at the E2–p7 junction (Δp7).

2.2. Monoclonal antibodies

Murine MAbs directed to HCV Core (#c11-7, #c11-10 and #c11-14), E1 (#299 and #384) and E2 (#187) were prepared against HCV aa 1–810 polyprotein expressed in insect cells (Matsuura et al., 1994; Takikawa et al., 2000). These MAbs are reactive in Western blot analysis. Murine anti-E1 MAb #159 (Triyatni et al., 2002) was kindly provided by J. Lau (Ribapharm, Inc.). Human MAbs directed to E1 (H-111 and H-114, unpublished) and E2 (CBH-2, 5, and 7; (Hadlock et al., 2000; Triyatni et al., 2002)) were derived from HCV-infected individuals and were kindly
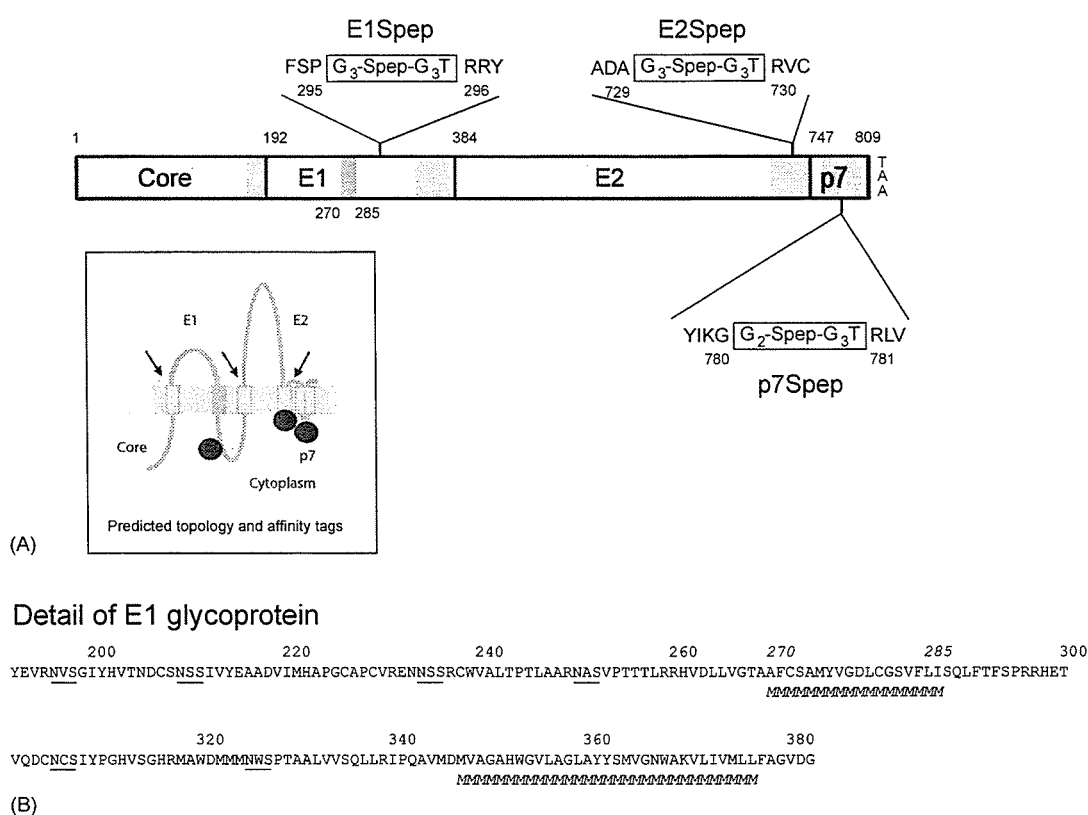
Fig. 1. The HCV structural polyprotein. (A) Schematic representation of the N-terminus encoding the Core, E1, E2 and p7 proteins; translation is terminated by an engineered termination codon (TAA) after p7. Amino acid numbering is shown, and transmembrane helical regions are indicated by shading. The putative internal transmembrane domain in E1 (aa 270–284) is darkened. The positions of the respective Spep tags are shown. The insert (lower left) contains a schematic showing the predicted membrane topology of the Core-E1-E2-p7 polyprotein including the polytopic form of the E1 glycoprotein. The respective Spep tags are shown as black balls. Arrows denote signal peptide cleavage sites in the polyprotein. (B) Amino acid sequence of the E1 glycoprotein. Transmembrane regions predicted by the PHD-htm algorithm (Rost et al., 1995); accessed at (Columbia University Bioinformatics Center, 2002) are indicated by M's under the amino acid sequence. Only extended regions identified with ≥90% probability are shown. Potential glycosylation sites are underlined.

provided by Z.-Y. Keck and S.K.H. Foung (Stanford University). Of these, only H-111 is able to recognize its respective protein in Western blot analysis (Z.-Y. Keck and S.K.H. Foung, unpublished). The other human MAbs recognize conformational determinants (Hadlock et al., 2000). Control studies utilized human MAbs directed against HIV-1 gp120 (447-52D, from S. Zolla-Pazner (Conley et al., 1994)) and gp41 (F240, from M. Posner (Cavacini et al., 1998)) and a murine anti-gp41 MAb (Chessie 8, from G. Lewis (Abacioglu et al., 1994)).

2.3. Characterization of affinity-tagged HCV glycoproteins

HCV expression plasmids were used to transiently transfect monkey COS cell using FuGENE-6 (Roche Biochemicals) reagent (Lu et al., 2001). In some experiments, cells were metabolically labeled for the final 16 h in 5 ml of cysteine- and methionine-free Dulbecco's Modified Eagle Medium containing 2% dialyzed fetal bovine serum and 125 μCi each ^{35}S-methionine and ^{35}S-cysteine (Amersham Life Sciences). Cells were har-

vested 48 h after transfection and lysed in solubilization buffer comprising 20 mM Tris–HCl, 100 mM ammonium sulfate, 10% glycerol (Mirzabekov et al., 2000), 0.5% cyclohexyl-pentyl-β-D-maltoside (Cymal-5; Anatrace, Maumee, OH) nonionic detergent and protease inhibitors (Complete Protease Inhibitor Tablets; Roche Diagnostics). Preliminary studies explored the use of other nonionic and zwitterionic detergents (Cymal-5, Triton X-100, Brij-97, and CHAPSO; 0.5% and 1%) and 0.5% Cymal-5 was chosen based on its efficiency in extracting noncovalently associated E1–E2 heterodimers and its high critical micellar concentration (to facilitate dialysis in the subsequent formation of proteoliposomes). In many studies, the solubilization buffer also contained 1 mM DTT (Tatu et al., 1993).

Spep-tagged proteins were isolated using S-protein agarose (SAG) beads (Novagen, Inc., Madison, WI). Briefly, cleared cell lysates (300–500 μl) were incubated with SAG beads (100 μl of slurry) at 4 °C for at least 1 h and the beads were subsequently washed in solubilization buffer. The affinity-purified material was typically eluted by boiling in Laemmli SDS-PAGE sample buffer, in the pres-

ence or absence of 100 mM DTT. Deglycosylation of the affinity-purified material using PNGase F (New England Biolabs, Beverly, MA) was performed as recommended by the manufacturer. Immunoprecipitation of Spep-tagged and untagged HCV envelope glycoproteins from cell lysates (500 μl) utilized 5 μg of the human MAbs. Immune complexes were precipitated using protein A–Sepharose (100 μl of a 50% v/v slurry; Sigma).

Proteins were resolved by SDS-PAGE and detected by phosphorimaging or by Western blot analysis using either S-protein horseradish peroxidase (S-HRP; Novagen, Inc.) or murine MAbs with an HRP-conjugated second antibody. Western blots were visualized by chemifluorescence using ECL-Plus (Amersham Biosciences) and quantitated by fluorescence imaging. Quantitative analyses were performed using the Fuji FLA3000G imager and Image Gauge software (Fuji).

2.4. S-protein paramagnetic beads and proteoliposomes

M-270 carboxylic acid Dynabeads (Dynal AS, Lake Success, NY) were activated using carbodiimide chemistry and coupled to S-protein (RNS2; Biozyme Laboratories, San Diego, CA) using methods recommended by Dynal AS. Spep-tagged HCV glycoproteins were isolated from cell lysates by overnight incubation with beads at 4 °C. Typically, 5×10^7 beads were used per 500 μl of cell lysate in order to obtain a dense coverage. The paramagnetic beads were subsequently washed extensively and maintained for up to 1 month in solubilization buffer at 4 °C. The nonionic detergent was included in all subsequent immunochemical analyses of the beads.

Lipids were obtained as chloroform solutions from Avanti Polar Lipids (Alabaster, AL). A total of 10 mg of lipids {1-palmitoyl-2-oleoyl-*sn*-glycero-3-phosphocholine (POPC), 1-palmitoyl-2-oleoyl-*sn*-glycero-3-phosphoethanolamine (POPE), and dimyristoylphosphatidic acid (DMPA), mixed in a molar ratio of 6:3:1} were dried in a glass vial under a vacuum until all of the solvent was removed. One milliliter of phosphate-buffered saline (PBS) was added to the tube, and a liposomal suspension was obtained by 1–2-min ultrasonication in an ice bath. A stock of the fluorescent lipid dioleoylphosphoethanolamine–lissamine rhodamine B (Rhodamine–DOPE) was similarly prepared, at a final concentration of 1 mg ml^{-1}, and used as a tracer to assess lipid accretion. All liposomal stocks were kept in liquid N_2 until use.

Proteoliposomes were produced using methods described by Sodroski and colleagues (Mirzabekov et al., 2000) and modified in our laboratory. In brief, the liposomal solution was added to a suspension of paramagnetic beads bearing the affinity-purified HCV envelope glycoproteins, and the Cymal-5 nonionic detergent was slowly removed by dialysis to enable proteoliposome formation. Considerable evidence supports the model that during solubilization, the nonionic detergent binds to transmembrane domains and

replaces the membrane; in reconstitution, this process is reversed (see review (Rigaud et al., 1995)). Fifty million paramagnetic beads and 50 μl of the 10 mg ml^{-1} liposome stock were mixed in 0.5 ml of solubilization buffer for 1 h at 4 °C before dialysis was initiated. Dialysis using a 10 kDa molecular weight cutoff cassette (Slide-A-Lyzer 10 K, Pierce, Rockford. IL) was carried out for 24 h at 4 °C against two changes of solubilization buffer lacking both detergent and protease inhibitors. Beads were then isolated magnetically and washed before storage in PBS containing 0.1% bovine serum albumin (BSA). Proteoliposome were stable for over 3 months at 4 °C, and were routinely washed into PBS (lacking BSA) prior to use.

Preliminary optimization and quality control studies for proteoliposome formation utilized the lipid mixture containing a tracer of Rhodamine–DOPE (1% w/w). Lipid was subsequently solubilized from the proteoliposomes and the amount of Rhodamine–DOPE tracer was determined spectrophotometrically. Approximately 60 μg of lipid could be deposited on 10^8 beads containing Spep-tagged transmembrane protein, sufficient to saturate the surface area of the beads (estimated at 50 μg (Mirzabekov et al., 2000)). Preliminary studies demonstrated that lipid accretion onto paramagnetic S-protein beads required that a transmembrane protein be bound (CTM and JHN; unpublished). Reports from numerous laboratories have demonstrated the robust utility of this methodology in reconstituting functional and antigenically intact transmembrane glycoproteins (see Babcock et al., 2001; Grundner et al., 2002; Mirzabekov et al., 2000; Rigaud et al., 1995; Walter et al., 1990).

2.5. Flow cytometric analysis of paramagnetic beads

Flow cytometry was performed using a FACSCalibur instrument (BD Biosciences). Paramagnetic beads ($\approx 5 \times 10^5$) containing affinity-purified HCV envelope glycoproteins in solubilization buffer (with 0.5% Cymal-5) or proteoliposomal beads ($\approx 5 \times 10^5$) in PBS and 0.1% BSA were incubated with 5 μg of the primary murine or human MAb in 50 μl for 1 h on ice and then washed in their respective buffers prior to incubation with the appropriate secondary antibody (CalTag, Burlingame, CA) at room temperature for 30 min. The murine MAbs were detected using a phycoerythrin-conjugated goat antibody, and the human MAbs were detected using a fluorescein-conjugated goat antibody. Both protein and proteoliposomal beads were ultimately washed into 1 ml of PBS for flow cytometric analysis.

3. Results

3.1. Selection of sites for affinity tags in the HCV envelope glycoproteins

In these studies, we sought to identify sites within E1, E2 and p7 that could accommodate the insertion of an affinity

tag without disrupting the biochemical and immunochemical properties of the noncovalently associated E1–E2 complex. We examined three sites with the potential for exposure on the cytosolic face of the membrane.

In the case of the polytopic p7 protein, which contains two hydrophobic membrane-spanning domains separated by a short cytoplasmic region (Carrere-Kremer et al., 2002), the affinity tag was introduced between charged amino acids in the cytoplasmic loop (Fig. 1A). Although the C-terminal regions of the E1 and E2 glycoproteins also contain charged amino acids embedded within hydrophobic transmembrane domains (Cocquerel et al., 2000), these residues are believed to lie within the membrane. It has been proposed that these charged residues play a role in reorienting the C-termini from the lumenal to cytosolic side of the ER following signal peptidase cleavage (Cocquerel et al., 2002; Op De Beeck et al., 2001). To explore this latter model in the E2 glycoprotein, we introduced the affinity tag between charged residues in the transmembrane domain of E2 (Fig. 1A), anticipating that this would severely disrupt biogenesis.

The E1 glycoprotein presented an unusual opportunity to probe structural and topologic aspects of biogenesis. Using predictive computer algorithms trained to identify transmembrane helices (Rost et al., 1995), we found evidence for a potential transmembrane helix internal to the E1 glycoprotein, between amino acid residues 270–284 (Fig. 1B). This raised the possibility that the E1 glycoprotein might contain two membrane-spanning regions — the well-documented C-terminal domain and the predicted internal domain — separated by an intervening cytoplasmic loop. This suggestion was consistent with earlier studies in which an internal hydrophobic region was shown to be involved in membrane association (Matsuura et al., 1994). Cytosolic exposure of the E1 glycoprotein has been suggested as the basis for interaction with the virion Core protein (Lo et al., 1996; Merola et al., 2001). Based on these theoretical and experimental suggestions, we introduced the affinity tag in the predicted cytoplasmic loop, between amino acids 295 and 296 (Fig. 1A).

3.2. Expression of the HCV envelope glycoproteins

The infectious HCV cDNA (genotype 1b) was originally isolated from an infected individual (Aizaki et al., 1998) and the region encoding the N-terminal polyprotein (Core, the E1 and E2 glycoproteins and p7) was used in these studies. The 15 amino acid S-peptide affinity tag (Spep) is derived from the small subtilisin-generated fragment of ribonuclease A and binds with high affinity to its ligand, the larger ribonuclease fragment (S-protein) (Kim and Raines, 1993; Richards and Vithayathil, 1959). This peptide was chosen based on its ability to function as an affinity tag when inserted internally within the protein of interest (JHN, unpublished). When transfected into simian COS-7 cells, the three tagged constructs (E1Spep, E2Spep and p7Spep; Fig. 1A) were expressed at levels comparable to the untagged
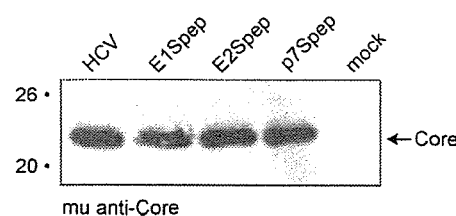

Fig. 2. Expression of HCV Core from Spep-tagged and untagged polyprotein. COS cells expressing the E1Spep, E2Spep or p7Spep polyproteins, or the untagged HCV polyprotein were lysed in solubilization buffer, and proteins were resolved by SDS-PAGE. The Western blot was probed using a pool of murine anti-Core MAbs (#c11-7, #c11-10 and #c11-14; indicated below the image as mu anti-Core). Molecular weight markers are shown at left.

HCV construct and all polyprotein expression resulted in the accumulation of proteolytically processed mature Core protein (Fig. 2).

We then examined the biosynthesis of the envelope glycoproteins to determine the effects of the affinity tag on protein processing, folding and assembly. Cells were lysed using 0.5% Cymal-5 nonionic detergent and the tagged glycoproteins were isolated using S-protein agarose (SAG) beads. In all cases, both E1 and E2 glycoproteins could be co-isolated, regardless of the position of the affinity tag (Fig. 3A). By far the highest recovery of E1–E2 complex was from the E1Spep polyprotein, and lower amounts were isolated from the p7Spep and E2Spep polyproteins, respectively. The expressed glycoproteins were further characterized by using peptide N-glycosidase F (PNGase F) to generate the fully deglycosylated proteins. In all cases, the E1 polypeptide was detected as a single band of the appropriate molecular weight (data not presented). The pattern of E2 polypeptides was, however, more complex (Fig. 3B). In the case of the E1Spep polyprotein, a discrete 40 kDa band corresponding to authentic E2 polypeptide was observed, as well as a series of more slowly migrating species. By contrast, the discrete band was absent in the E2Spep and p7Spep polyprotein products and only the more slowly migrating species were seen. Based on previous reports (Lin et al., 1994; Mizushima et al., 1994), we suspected that one or more of the slowly migrating species might represent unprocessed E2–p7 precursor. To further examine this question, we modified the E1Spep construct by introducing a stop codon at the E2–p7 junction to ablate expression of p7. The slowly migrating species vanished and only the authentic E2 polypeptide remained (Fig. 3C). These results confirm that the more slowly migrating species represent forms of the uncleaved E2–p7 precursor. Therefore, we concluded that the E2Spep and p7Spep polyproteins were largely defective in signal peptidase cleavage at the E2–p7 junction. By contrast, the E1Spep polyprotein was able to undergo proteolytic processing to yield mature E1 and E2 glycoproteins.

To assess the state of protein folding in the E1Spep-E2 complex, we examined the mobility of the E2 glycoprotein by SDS-polyacrylamide gel electrophoresis (SDS-PAGE)
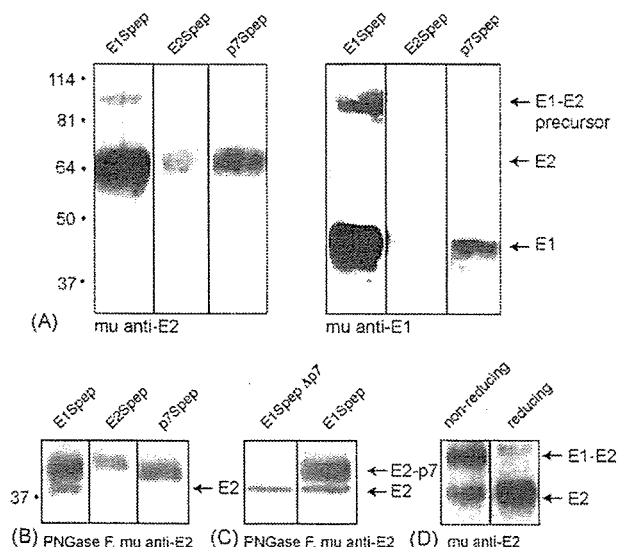
(A) Reducing SDS-PAGE   (B) Non-reducing SDS-PAGE

Fig. 3. Characterization of Spep-tagged HCV envelope glycoproteins. Expressed proteins were precipitated using S-protein agarose (SAG) and Western blots were visualized using murine MAbs directed to either E1 (MAbs #299 and #384) or E2 (MAbs #187) as indicated below the image (mu anti-E1 or mu anti-E2, respectively). Molecular weight markers are indicted at left. (A) Isolation by SAG precipitation of E2 (left) and E1 (right) from cells expressing E1Spep, E2Spep and p7Spep. The mature E1 and E2 glycoproteins are indicated at right; residual unprocessed E1–E2 precursor is also visible. (B) Isolated glycoproteins were deglycosylated using PNGase F and E2-reactive polypeptides were detected using murine anti-E2 MAb. The expected position of the E2 polypeptide is indicated. (C) p7 Expression was ablated from the E1Spep polyprotein by introducing a stop codon at the E2–p7 junction (E1SpepΔp7). Glycoproteins were deglycosylated using PNGase F and E2 polypeptides were detected using murine anti-E2 MAb. E2 and E2–p7 polypeptides are indicated. (D) The E1–E2 complex from E1Spep polyprotein was isolated and resolved by SDS-PAGE under non-reducing or reducing conditions. The E2 glycoprotein and the disulfide-crosslinked E1–E2 complex are indicated.
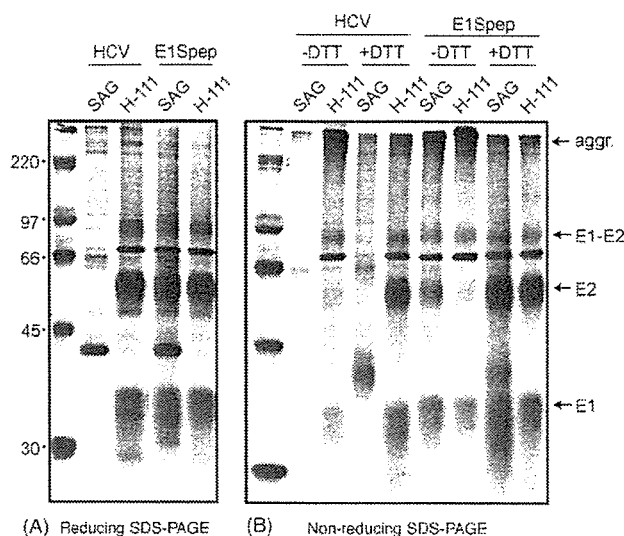
Fig. 4. Isolation of noncovalently associated E1–E2 complex under mildly reducing conditions. Cells expressing the untagged HCV structural polyprotein or the E1Spep polyprotein were metabolically labeled using ^{35}S-methionine and -cysteine and lysed in solubilization buffer with (+DTT) or without (−DTT) 1 mM DTT. E1–E2 complexes were precipitated using either SAG or a human anti-E1 MAb H-111. Isolated proteins were resolved by SDS-PAGE under reducing (A) or non-reducing (B) conditions. Free E1 and E2 are indicated, as are the covalently linked E1–E2 complex/precursor (E1–E2) and the higher molecular weight aggregates (aggr.). Cells expressing the untagged HCV polyprotein served as control for the SAG precipitation. ^{14}C-labeled molecular weight markers (Amersham Biosciences) are shown at left. The identity of the additional bands (≈ 40 and 70 kDa) is unknown.

under nonreducing conditions. In these experiments, the misfolded disulfide-crosslinked E1–E2 complex migrates slowly, whereas the noncovalently associated E2 migrates as the free glycoprotein. From these studies (Fig. 3D), we estimated that ≈25% of the E2 glycoprotein isolated by using the E1Spep tag was in the form of noncovalently associated complex. Although this percentage is similar to that reported for the untagged HCV polyproteins (Deleersnyder et al., 1997; Dubuisson et al., 1994; Dubuisson and Rice, 1996 and see below), we were surprised at the extent of apparent misfolding.

In order to investigate the source of the disulfide-crosslinked aggregates commonly found upon expression of the HCV envelope glycoproteins, we modified our cell lysis buffer to include 1 mM DTT. We reasoned that this low level of reducing agent might mitigate against the oxidative environment in the ER (Tatu et al., 1993) but would itself be unable to reduce properly folded protein. If proper folding of the expressed glycoproteins were limited kinetically, then this low level of reducing agent might enhance the isolation of properly folded, noncovalently associated

complex. We explored this hypothesis using both the native, untagged HCV structural polyprotein and the affinity-tagged E1Spep polyprotein. Cells were metabolically labeled and lysed in the presence or absence of 1 mM DTT. Complexes were then immunoprecipitated using either SAG, or a human anti-E1 MAb H-111 (Z.-Y. Keck and S.K.H. Foung; unpublished). Overall yields were similar in the presence or absence of DTT and lysis in the presence of 1 mM DTT did not disrupt the E1–E2 association (Fig. 4A). As analyzed by SDS-PAGE under reducing conditions, comparable amounts of E1–E2 complex were isolated by H-111 from cells expressing the tagged or untagged HCV polyprotein, suggesting retention of the MAb epitope. Importantly, both tagged and untagged complexes isolated in the presence of 1 mM DTT were largely noncovalently associated (Fig. 4B). By contrast, samples prepared in the absence of 1 mM DTT showed significant amounts of E1–E2 aggregation, and commensurately lesser amounts of noncovalently associated E1 and E2.

We speculate that lysis under mildly reducing conditions may prevent artefactual disulfide bond formation during isolation or, more likely, may facilitate disulfide bond reshuffling in the nascent complex. We presume that, in the absence of competing and irreversible disulfide bond formation, the glycoprotein complex in the presence of 1 mM DTT is able to fold into its native state.
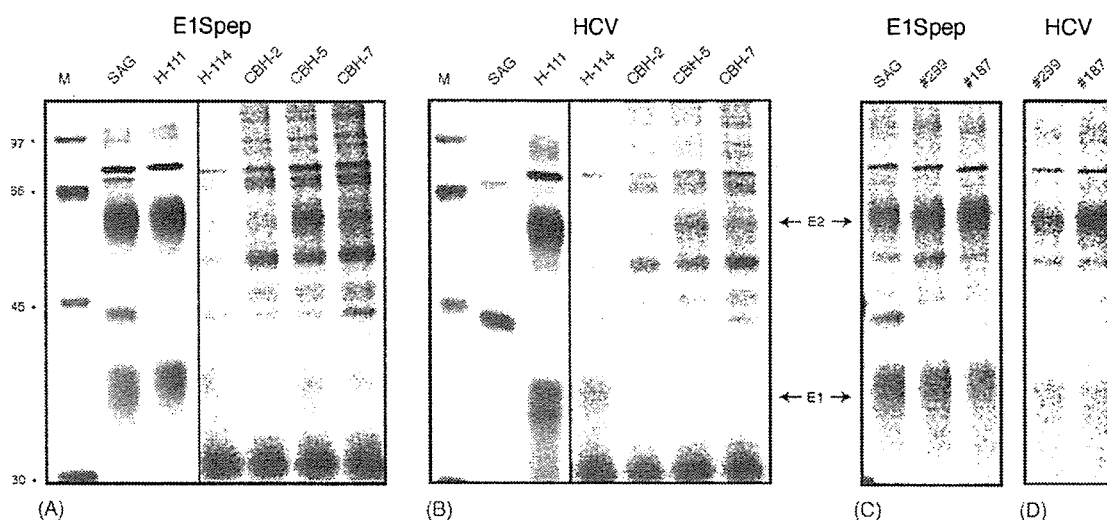
Fig. 5. Immunoprecipitation of E1–E2 complexes. Cells expressing the E1Spep (panels A and C) or the untagged HCV (panels B and D) polyprotein were metabolically labeled and lysed in solubilization buffer containing 1 mM DTT. Complexes were precipitated using the indicated reagents: SAG, human anti-E1 MAbs H-111 or H-114, human anti-E2 MAbs CBH-2, CBH-5 or CBH-7, or with murine anti-E1 MAb #299 or murine anti-E2 MAb #187. (A) Isolation of E1Spep-E2 complex using human MAbs. The image representing SAG and H-111 has been significantly lightened relative to that of the other human MAbs. Quantitation of radioactivity revealed that, relative to H-111, CBH-2 was able to precipitate 2% of the E2 glycoprotein, CBH-5 (13%), and CBH-7 (11%). Significant amounts were not detected using H-114. (B) Isolation of E1–E2 complex from untagged HCV polyprotein. Lanes representing SAG and H-111 are significantly lightened. Relative yields of E2 glycoprotein for CBH-5 and CBH-7 were 6 and 5%, respectively; no significant amounts of E2 were detected using H-114 or CBH-2. (C) and (D) Isolation of, respectively, E1Spep and HCV complex using murine MAbs #299 and #187.

3.3. Monoclonal antibodies as structural probes

To further assess the structural integrity of the noncovalently associated complex, we examined the ability of MAbs to recognize the solubilized glycoproteins. As depicted in Fig. 5, E1–E2 complex from cells expressing either the tagged or untagged HCV structural polyproteins was readily immunoprecipitated by murine MAbs directed against linear epitopes in either E1 or E2 (#299 and #187, respectively) and by the human anti-E1 MAb H-111. A significantly lesser amount of E1–E2 complex was isolated using conformation-dependent human MAbs directed to E1 (MAb H-114; Z.-Y. Keck and S.K.H. Foung, unpublished) or E2 (MAbs CBH-2, CBH-5 and CBH-7 (Hadlock et al., 2000; Triyatni et al., 2002)). Although these anti-E2 MAbs were isolated from a patient infected with a genotype 1b virus (Hadlock et al., 2000), we were able to recover at most 13% of the E1–E2 complex of this genotype 1b isolate. In other experiments, a similar pattern of reactivity was observed using complexes prepared in the absence of 1 mM DTT (data not shown). The overall diminution in reactivity of these human MAbs may be ascribed to antigenic differences between the virus of the MAb donor and those represented in the expression plasmid, or to conformational differences in the isolated complex. Importantly, however, the pattern of MAb reactivity was identical using complexes derived from the tagged and untagged HCV polyprotein. These parallels suggest that the immunochemical structure of the complex was not grossly perturbed by the introduction of the affinity tag.

Further attempts to ascertain the integrity of the complexes using a soluble form of the putative HCV receptor CD81 (Flint et al., 1999) were uninformative in that CD81 does not bind to genotype 1b glycoproteins (Roccasecca et al., 2003; Triyatni et al., 2002; Yagnik et al., 2000).

3.4. MAb binding to affinity-captured E1Spep–E2 complex and proteoliposomes

Taken together, our analyses suggested that assembly of the E1–E2 complex was largely unaffected by the introduction of the affinity tag at position 295/296 in E1. Based on computer predictions that the E1 glycoprotein may be able to adopt a polytopic topology in which the Spep-tagged region would lie on the cytoplasmic side of the membrane, we sought to reconstruct the predicted topology of the E1Spep glycoprotein by generating affinity-captured and properly oriented proteoliposomal complexes. We first used S-protein-conjugated paramagnetic beads to isolate E1Spep–E2 complex. Bound E1Spep was readily detected by flow cytometry using murine anti-E1 MAbs or the human MAbs H-111 (Fig. 6A) and associated E2 glycoprotein was demonstrated by Western blot analysis using the anti-E2 MAb #187 (Fig. 6B). The nonionic detergent was then replaced with a liposomal membrane to examine membrane topology. Because lipid accretion occurs at transmembrane regions of the bound proteins, continued exposure of E1 and E2 epitopes upon reconstitution would suggest that the ectodomains of E1 and E2 are properly oriented in the proteoliposome, despite anchoring by the affinity tag.
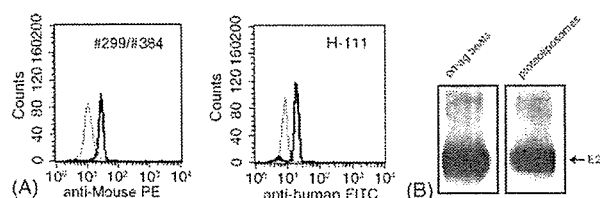
Fig. 6. Analysis of E1Spep and E2 glycoproteins on paramagnetic beads and proteoliposomes. S-protein coupled Dynabeads were used to isolate E1–E2 complex from lysates of cells expressing the E1Spep polyprotein. (A) Flow cytometric analysis of paramagnetic beads. Beads were incubated with anti-E1 MAbs in buffer containing 0.5% Cymal-5 nonionic detergent. Murine MAbs #299 and #384 (pooled) were detected using a second antibody labeled with phycoerythrin (PE); human MAb H-111 was detected using a second antibody labeled with fluorescein isothiocyanate (FITC). Histograms are shown in black lines. The negative control (filled, gray histograms) for the murine MAbs are paramagnetic beads bearing Spep-tagged CD4 (Gallina et al., 2002) and stained using the murine anti-E1 MAbs; the negative control for the human MAb are E1Spep paramagnetic beads stained using the anti-HIV MAb 447-52D (Conley et al., 1994). (B) Western blot analysis of E2 glycoprotein captured via E1Spep on paramagnetic beads (pmag beads) and subsequently retained in proteoliposomes. Lysates were prepared in solubilization buffer containing 1 mM DTT and bound E2 glycoprotein was detected using non-reducing SDS-PAGE and murine anti-E2 MAb #187.

Using protocols derived from Sodroski and colleagues (Babcock et al., 2001; Grundner et al., 2002; Mirzabekov et al., 2000), a mixture of synthetic lipids was added to the suspension of paramagnetic beads bearing the E1Spep–E2 complex, and the Cymal-5 nonionic detergent was then removed by dialysis to allow formation of the proteoliposomal membrane. Lipid accretion was sufficient to cover the paramagnetic bead, albeit not necessarily as a continuous membrane (see Section 2), and biochemical analysis of the reconstituted E1Spep–E2 proteoliposomes showed complete retention of the noncovalently associated E2 glycoprotein (Fig. 6B). Proteoliposomes constructed in this manner have, in many cases, been shown to display properly oriented and correctly folded glycoproteins (Grundner et al., 2002; Mirzabekov et al., 2000; Rigaud et al., 1995; Walter et al., 1990; CTM and JHN, unpublished).

Murine and human MAbs that recognized the detergent-solubilized E1Spep–E2 complex also recognized the proteoliposomal complex (Fig. 7). Linear epitopes within the E1 glycoprotein remained accessible to binding by murine MAbs #299 and #384, and #159 (kindly provided by J. Lau; (Triyatni et al., 2002)) and by the human anti-E1 MAb H-111. The retention of E1 glycoprotein exposure and reactivity, despite saturating amounts of lipid, is consistent with formation of the lipid bilayer between the ectodomain and the Spep anchor on the bead. Accretion of even a discontinuous bilayer at a single, C-terminal transmembrane domain would be anticipated to occlude antibody access to the now-buried ectodomain. In fact, binding to the proteoliposomes was comparable to that seen with the same paramagnetic beads prior to membrane accretion (see Fig. 6). The proteoliposomal E2 glycoprotein also remained accessible to murine MAb #187. As anticipated, little or no

binding was detected using human MAbs that only weakly recognized the solubilized complexes (H-114, CBH-2, CBH-5 and CBH-7; Fig. 7).

Taken together, these studies suggest that the immunochemical properties of the E1Spep–E2 complex were unchanged by membrane reconstitution. These results are consistent with the prediction that E1 glycoprotein can assume a polytopic topology consisting of two membrane-spanning domains — the internal and C-terminal transmembrane regions — and an intervening cytoplasmic loop. In our studies with proteoliposomes, this topology was enforced by the Spep affinity tag. The parallel immune reactivity of the tagged and untagged glycoproteins in solution, however, suggests that the E1 glycoprotein may naturally display flexibility in its folding and membrane topology.

4. Discussion

Our studies suggest that the HCV E1 glycoprotein is able to adopt a polytopic topology in which the heterodimeric noncovalent association with the E2 glycoprotein subunit is retained. Further studies are clearly needed to prove the existence of this alternative form, and to define its relationship to the canonical, Type I form of the E1 glycoprotein. In the absence of a productive cell culture system for the growth of infectious HCV, direct links between envelope glycoprotein structure and function are difficult to demonstrate. In fact, a firm definition of the native structure(s) of the HCV envelope glycoproteins remains elusive despite the recent development of infectious pseudotyped virions bearing the E1–E2 complex (Bartosch et al., 2003; Drummer et al., 2003; Hsu et al., 2003). Nonetheless, our studies highlight the possibility that the E1 glycoprotein is capable of topologic flexibility.

In considering a cytoplasmic loop in the E1 glycoprotein (amino acids 285–344), it is perhaps significant that the potential glycosylation site at amino acid 325 is not utilized in the wild-type E1 glycoprotein (Meunier et al., 1999). Mutation to a more optimal glycosylation motif (NWSP to NTSG) enables only partial utilization of this site (Meunier et al., 1999). It is unclear whether the unglycosylated fraction reflects suboptimal glycosylation or a mixture of E1 topologies. Similarly, although the glycosylation site at position 305 appears to be utilized in some E1 glycoproteins (Meunier et al., 1999), this position is variably glycosylated in the genotype 1b isolate used here (YM, unpublished).

Topologic flexibility during biogenesis has been reported for other viral envelope glycoproteins. In the case of Hepatitis B virus, the surface glycoprotein is initially formed in the ER with the entire pre-S domain located in the cytosol; during maturation, 50% of the glycoprotein is converted to an alternative topology wherein the pre-S domain is translocated through the membrane to the lumenal side (Lambert and Prange, 2001 and references therein). Recently, Morri-
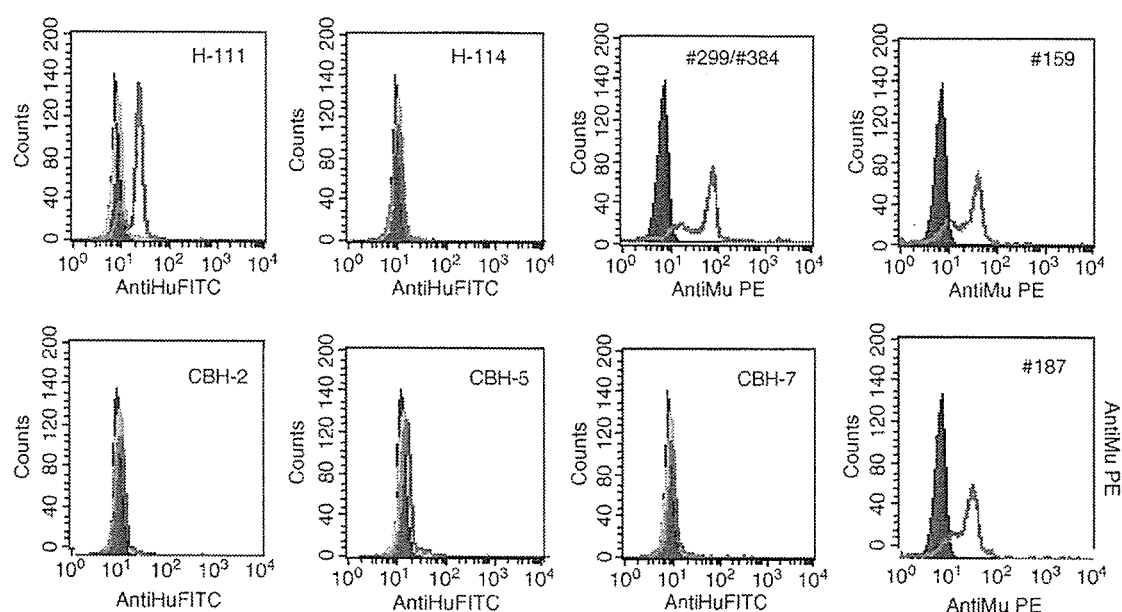
Fig. 7. Flow cytometric analysis of MAb binding to proteoliposomal E1–E2 complexes. Proteoliposomal beads were incubated with the indicated human or murine MAbs and subsequently stained using the appropriate secondary antibody conjugated, respectively, to FITC or PE. The murine anti-E1 MAb #159 was kindly provided by J. Lau (Triyatni et al., 2002). Control human MAbs directed to irrelevant antigens (HIV envelope glycoprotein gp120 and gp41, respectively) were kindly provided by S. Zolla-Pazner and M. Posner. A murine anti-gp41 MAb served as negative control for the murine anti-HCV MAbs and was kindly provided by G. Lewis. Histograms of anti-HCV MAb binding are shown by gray lines; control anti-HIV MAbs are shown in solid black histograms. For MAb H-111, the absence of binding to HIV-1 gp160 proteoliposomal beads (unpublished) is indicated in gray within the negative peak. The source of the minor, dull peak seen using the murine anti-HCV MAbs is unclear.

son and colleagues have reported that the fusion glycoprotein of Newcastle disease virus (NDV), for which a Type I membrane topology is well documented, can also assume a polytopic topology (McGinnes et al., 2003). The specific polytopic topology of the NDV fusion glycoprotein is similar to that which we propose for the HCV E1 glycoprotein.

If a cytoplasmic loop of E1 is involved in interactions with the virion core, as has been suggested (Lo et al., 1996; Merola et al., 2001), the immunochemical significance of an alternative form of the E1–E2 complex is unknown. In this regard, it is perhaps noteworthy that the human MAbs that weakly bind the E1–E2 complex in our studies have previously been described as broad in their specificity, recognizing determinants conserved between genotypes 1a and 1b (Hadlock et al., 2000). In other studies, however, gaps in this broad pattern of recognition have been observed (Cocquerel et al., 2003; Triyatni et al., 2002). The immunochemical differences noted in the literature may well be related to the genetic diversity among isolates or to the cell culture system used for recombinant expression. Based on our studies, we suggest that antigenic differences may also reflect the topologic flexibility of the HCV E1 glycoprotein. Although we cannot explain the apparent preference for the polytopic form in our studies, our findings raise the possibility that the topologic flexibility of the HCV E1 glycoprotein may play a role in immune evasion.

One might imagine that topologic flexibility in the E1–E2 complex could serve to direct the antibody response away from critical and conserved elements of the viral envelope spike. This concept has been best advanced in the case of the HIV envelope glycoprotein, where the antibody response is directed predominantly to variable epitopes displayed only on the monomeric gp120 subunit (Moore and Ho, 1995; Parren et al., 1997; Parren et al., 1999). Epitopes that give rise to rare broadly neutralizing anti-HIV MAbs appear to be physically and conformationally occluded within the oligomeric gp120–gp41 complex (Cao et al., 1997; Kwong et al., 2002; Saphire et al., 2001; Wyatt et al., 1995). By exposing antigenically variable determinants and minimizing conserved epitopes, HIV and HCV may be utilizing a common strategy, albeit via distinct mechanisms, to evade the immune response towards the establishment of chronic infection.

The task of designing an effective and much-needed HCV vaccine is complicated by the paucity of knowledge regarding the structure and function of the native HCV envelope glycoprotein complex. Recently, several laboratories have reported that infectious pseudotyped virions bearing the HCV E1–E2 complex can be generated in cell culture (Bartosch et al., 2003; Drummer et al., 2003; Hsu et al., 2003) and it is possible that this methodology may be refined to enable the biochemical and immunochemical dissection of the functional HCV envelope glycoprotein complex. In this regard, it may be important to consider the role of an alternative E1 glycoprotein topology in HCV biology and pathogenesis.

Acknowledgements

References

Abacioglu, Y.H., Fouts, T.R., Laman, J.D., Claassen, E., Pincus, S.H., Moore, J.P., Roby, C.A., Kamin-Lewis, R., Lewis, G.K., 1994. Epitope mapping and topology of baculovirus-expressed HIV-1 gp160 determined with a panel of murine monoclonal antibodies. AIDS Res. Hum. Retroviruses 10, 371–381.

Aizaki, H., Aoki, Y., Harada, T., Ishii, K., Suzuki, T., Nagamori, S., Toda, G., Matsuura, Y., Miyamura, T., 1998. Full-length complementary DNA of hepatitis C virus genome from an infectious blood sample. Hepatology 27, 621–627.

Babcock, G.J., Mirzabekov, T., Wojtowicz, W., Sodroski, J., 2001. Ligand-binding characteristics of CXCR4 incorporated into paramagnetic proteoliposomes. J. Biol. Chem. 276, 38,433–38,440.

Bartenschlager, R., Lohmann, V., 2001. Novel cell culture systems for the hepatitis C virus. Antiviral Res. 52, 1–17.

Bartosch, B., Dubuisson, J., Cosset, F.L., 2003. Infectious hepatitis C virus pseudo-particles containing functional E1–E2 envelope protein complexes. J. Exp. Med. 197, 633–642.

Cao, J., Sullivan, N., Desjardin, E., Parolin, C., Robinson, J., Wyatt, R., Sodroski, J., 1997. Replication and neutralization of human immunodeficiency virus type 1 lacking the V1 and V2 variable loops of the gp120 envelope glycoprotein. J. Virol. 71, 9808–9812.

Carrere-Kremer, S., Montpellier-Pala, C., Cocquerel, L., Wychowski, C., Penin, F., Dubuisson, J., 2002. Subcellular localization and topology of the p7 polypeptide of hepatitis C virus. J. Virol. 76, 3720–3730.

Cavacini, L.A., Emes, C.L., Wisnewski, A.V., Power, J., Lewis, G., Montefiori, D., Posner, M.R., 1998. Functional and molecular characterization of human monoclonal antibody reactive with the immunodominant region of HIV type 1 glycoprotein 41. AIDS Res. Hum. Retroviruses 14, 1271–1280.

Choukhi, A., Ung, S., Wychowski, C., Dubuisson, J., 1998. Involvement of endoplasmic reticulum chaperones in the folding of hepatitis C virus glycoproteins. J. Virol. 72, 3851–3858.

Cocquerel, L., Meunier, J.C., Pillez, A., Wychowski, C., Dubuisson, J., 1998. A retention signal necessary and sufficient for endoplasmic reticulum localization maps to the transmembrane domain of hepatitis C virus glycoprotein E2. J. Virol. 72, 2183–2191.

Cocquerel, L., Duvet, S., Meunier, J.C., Pillez, A., Cacan, R., Wychowski, C., Dubuisson, J., 1999. The transmembrane domain of hepatitis C virus glycoprotein E1 is a signal for static retention in the endoplasmic reticulum. J. Virol. 73, 2641–2649.

Cocquerel, L., Wychowski, C., Minner, F., Penin, F., Dubuisson, J., 2000. Charged residues in the transmembrane domains of hepatitis C virus glycoproteins play a major role in the processing, subcellular localization, and assembly of these envelope proteins. J. Virol. 74, 3623–3633.

Cocquerel, L., Op de Beeck, A., Lambot, M., Roussel, J., Delgrange, D., Pillez, A., Wychowski, C., Penin, F., Dubuisson, J., 2002. Topological changes in the transmembrane domains of hepatitis C virus envelope glycoproteins. EMBO J. 21, 2893–2902.

Cocquerel, L., Quinn, E.R., Flint, M., Hadlock, K.G., Foung, S.K., Levy, S., 2003. Recognition of native hepatitis C virus E1E2 heterodimers by a human monoclonal antibody. J. Virol. 77, 1604–1609.

Columbia University Bioinformatics Center, 2002. PredictProtein.

Conley, A.J., Gorny, M.K., Kessler II, J.A., Boots, L.J., Ossorio-Castro, M., Koenig, S., Lineberger, D.W., Emini, E.A., Williams, C., Zolla-Pazner, S., 1994. Neutralization of primary human immunodeficiency virus type 1 isolates by the broadly reactive anti-V3 monoclonal antibody, 447-52D. J. Virol. 68, 6994–7000.

Deleersnyder, V., Pillez, A., Wychowski, C., Blight, K., Xu, J., Hahn, Y.S., Rice, C.M., Dubuisson, J., 1997. Formation of native hepatitis C virus glycoprotein complexes. J. Virol. 71, 697–704.

Drummer, H.E., Maerz, A., Poumbourios, P., 2003. Cell surface expression of functional hepatitis C virus E1 and E2 glycoproteins. FEBS Lett. 546, 385–390.

Dubuisson, J., 2000. Folding, assembly and subcellular localization of hepatitis C virus glycoproteins. Curr. Top. Microbiol. Immunol. 242, 135–148.

Dubuisson, J., Hsu, H.H., Cheung, R.C., Greenberg, H.B., Russell, D.G., Rice, C.M., 1994. Formation and intracellular localization of hepatitis C virus envelope glycoprotein complexes expressed by recombinant vaccinia and Sindbis viruses. J. Virol. 68, 6147–6160.

Dubuisson, J., Rice, C.M., 1996. Hepatitis C virus glycoprotein folding: disulfide bond formation and association with calnexin. J. Virol. 70, 778–786.

Duvet, S., Cocquerel, L., Pillez, A., Cacan, R., Verbert, A., Moradpour, D., Wychowski, C., Dubuisson, J., 1998. Hepatitis C virus glycoprotein complex localization in the endoplasmic reticulum involves a determinant for retention and not retrieval. J. Biol. Chem. 273, 32,088–32,095.

Flint, M., Maidens, C., Loomis-Price, L.D., Shotton, C., Dubuisson, J., Monk, P., Higginbottom, A., Levy, S., McKeating, J.A., 1999. Characterization of hepatitis C virus E2 glycoprotein interaction with a putative cellular receptor, CD81. J. Virol. 73, 6235–6244.

Flint, M., McKeating, J.A., 1999. The C-terminal region of the hepatitis C virus E1 glycoprotein confers localization within the endoplasmic reticulum. J. Gen. Virol. 80, 1943–1947.

Gallina, A., Hanley, T.M., Mandel, R., Trahey, M., Broder, C.C., Viglianti, G.A., Ryser, H.J., 2002. Inhibitors of protein-disulfide isomerase prevent cleavage of disulfide bonds in receptor-bound glycoprotein 120 and prevent HIV-1 entry. J. Biol. Chem. 277, 50,579–50,588.

Grakoui, A., Wychowski, C., Lin, C., Feinstone, S.M., Rice, C.M., 1993. Expression and identification of hepatitis C virus polyprotein cleavage products. J. Virol. 67, 1385–1395.

Grundner, C., Mirzabekov, T., Sodroski, J., Wyatt, R., 2002. Solid-phase proteoliposomes containing human immunodeficiency virus envelope glycoproteins. J. Virol. 76, 3511–3521.

Hadlock, K.G., Lanford, R.E., Perkins, S., Rowe, J., Yang, Q., Levy, S., Pileri, P., Abrignani, S., Foung, S.K., 2000. Human monoclonal antibodies that inhibit binding of hepatitis C virus E2 protein to CD81 and recognize conserved conformational epitopes. J. Virol. 74, 10,407–10,416.

Hsu, M., Zhang, J., Flint, M., Logvinoff, C., Cheng-Mayer, C., Rice, C.M., McKeating, J.A., 2003. Hepatitis C virus glycoproteins mediate pH-dependent cell entry of pseudotyped retroviral particles. Proc. Natl. Acad. Sci. U. S. A. 100, 7271–7276.

Kim, J.-S., Raines, R.T., 1993. Ribonuclease S-peptide as a carrier in fusion proteins. Prot. Sci. 2, 348–356.

Kwong, P.D., Doyle, M.L., Casper, D.J., Cicala, C., Leavitt, S.A., Majeed, S., Steenbeke, T.D., Venturi, M., Chaiken, I., Fung, M., Katinger, H., Parren, P.W., Robinson, J., Van Ryk, D., Wang, L., Burton, D.R., Freire, E., Wyatt, R., Sodroski, J., Hendrickson, W.A., Arthos, J., 2002. HIV-1 evades antibody-mediated neutralization through conformational masking of receptor-binding sites. Nature 420, 678–682.

Lambert, C., Prange, R., 2001. Dual topology of the hepatitis B virus large envelope protein: determinants influencing post-translational pre-S translocation. J. Biol. Chem. 276, 22,265–22,272.

Lin, C., Lindenbach, B.D., Pragai, B.M., McCourt, D.W., Rice, C.M., 1994. Processing in the hepatitis C virus E2-NS2 region: identification of p7 and two distinct E2-specific products with different C termini. J. Virol. 68, 5063–5073.

Lo, S.Y., Selby, M.J., Ou, J.H., 1996. Interaction between hepatitis C virus core protein and E1 envelope protein. J. Virol. 70, 5177–5182.

Lu, M., Stoller, M.O., Wang, S., Liu, J., Fagan, M.B., Nunberg, J.H., 2001. Structural and functional analysis of interhelical interactions in the HIV-1 gp41 envelope glycoprotein by alanine-scanning mutagenesis. J. Virol. 75, 11,146–11,156.

Matsuura, Y., Suzuki, T., Suzuki, R., Sato, M., Aizaki, H., Saito, I., Miyamura, T., 1994. Processing of E1 and E2 glycoproteins of hepatitis C virus expressed in mammalian and insect cells. Virology 205, 141–150.

McGinnes, L.W., Reitter, J.N., Gravel, K., Morrison, T.G., 2003. Evidence for mixed membrane topology of the Newcastle disease virus fusion protein. J. Virol. 77, 1951–1963.

Merola, M., Brazzoli, M., Cocchiarella, F., Heile, J.M., Helenius, A., Weiner, A.J., Houghton, M., Abrignani, S., 2001. Folding of hepatitis C virus E1 glycoprotein in a cell-free system. J. Virol. 75, 11,205–11,217.

Meunier, J.C., Fournillier, A., Choukhi, A., Cahour, A., Cocquerel, L., Dubuisson, J., Wychowski, C., 1999. Analysis of the glycosylation sites of Hepatitis C virus (HCV) glycoprotein E1 and the influence of E1 glycans on the formation of the HCV glycoprotein complex. J. Gen. Virol. 80, 887–896.

Michalak, J.P., Wychowski, C., Choukhi, A., Meunier, J.C., Ung, S., Rice, C.M., Dubuisson, J., 1997. Characterization of truncated forms of hepatitis C virus glycoproteins. J. Gen. Virol. 78, 2299–2306.

Mirzabekov, T., Kontos, H., Farzan, M., Marasco, W., Sodroski, J., 2000. Paramagnetic proteoliposomes containing a pure, native, and oriented seven-transmembrane segment protein, CCR5. Nat. Biotech. 18, 649–654.

Mizushima, H., Hijikata, M., Asabe, S., Hirota, M., Kimura, K., Shimotohno, K., 1994. Two hepatitis C virus glycoprotein E2 products with different C termini. J. Virol. 68, 6215–6222.

Moore, J.P., Ho, D.D., 1995. HIV-1 neutralization: the consequences of viral adaptation to growth on transformed T cells. AIDS 9 (Suppl. A), S117–S136.

Op De Beeck, A., Montserret, R., Duvet, S., Cocquerel, L., Cacan, R., Barberot, B., Le Maire, M., Penin, F., Dubuisson, J., 2000. The transmembrane domains of hepatitis C virus envelope glycoproteins E1 and E2 play a major role in heterodimerization. J. Biol. Chem. 275, 31,428–31,437.

Op De Beeck, A., Cocquerel, L., Dubuisson, J., 2001. Biogenesis of hepatitis C virus envelope glycoproteins. J. Gen. Virol. 82, 2589–2595.

Parren, P.W., Gauduin, M.C., Koup, R.A., Poignard, P., Sattentau, Q.J., Fisicaro, P., Burton, D.R., 1997. Relevance of the antibody response against human immunodeficiency virus type 1 envelope to vaccine design. Immunol. Lett. 58, 125–132.

Parren, P.W.H.I., Moore, J.P., Burton, D.R., Sattentau, Q.J., 1999. The neutralizing antibody response to HIV-1: viral evasion and escape from humoral immunity. AIDS 13 (Suppl. A), S137–S162.

Patel, J., Patel, A.H., McLauchlan, J., 2001. The transmembrane domain of the hepatitis C virus E2 glycoprotein is required for correct folding of the E1 glycoprotein and native complex formation. Virology 279, 58–68.

Reed, K.E., Rice, C.M., 2000. Overview of hepatitis C virus genome structure, polyprotein processing, and protein properties. Curr. Top. Microbiol. Immunol. 242, 55–84.

Richards, F.M., Vithayathil, P.J., 1959. The preparation of subtilisin-modified ribonuclease and the separation of the peptide and protein components. J. Biol. Chem. 234, 1459–1465.

Rigaud, J.L., Pitard, B., Levy, D., 1995. Reconstitution of membrane proteins into liposomes: application to energy-transducing membrane proteins. Biochem. Biophys. Acta 1231, 223–246.

Roccasecca, R., Ansuini, H., Vitelli, A., Meola, A., Scarselli, E., Acali, S., Pezzanera, M., Ercole, B.B., McKeating, J., Yagnik, A., Lahm, A., Tramontano, A., Cortese, R., Nicosia, A., 2003. Binding of the hepatitis C virus E2 glycoprotein to CD81 is strain specific and is modulated by a complex interplay between hypervariable regions 1 and 2. J. Virol. 77, 1856–1867.

Rost, B., Casadio, R., Fariselli, P., Sander, C., 1995. Transmembrane helices predicted at 95% accuracy. Prot. Sci. 4, 521–533.

Saphire, E.O., Parren, P.W., Pantophlet, R., Zwick, M.B., Morris, G.M., Rudd, P.M., Dwek, R.A., Stanfield, R.L., Burton, D.R., Wilson, I.A., 2001. Crystal structure of a neutralizing human IGG against HIV-1: a template for vaccine design. Science 293, 1155–1159.

Selby, M.J., Choo, Q.L., Berger, K., Kuo, G., Glazer, E., Eckart, M., Lee, C., Chien, D., Kuo, C., Houghton, M., 1993. Expression, identification and subcellular localization of the proteins encoded by the hepatitis C viral genome. J. Gen. Virol. 74, 1103–1113.

Takikawa, S., Ishii, K., Aizaki, H., Suzuki, T., Asakura, H., Matsuura, Y., Miyamura, T., 2000. Cell fusion activity of hepatitis C virus envelope proteins. J. Virol. 74, 5066–5074.

Tatu, U., Braakman, I., Helenius, A., 1993. Membrane glycoprotein folding, oligomerization and intracellular transport: effects of dithiothreitol in living cells. EMBO J. 12, 2151–2157.

Triyatni, M., Vergalla, J., Davis, A.R., Hadlock, K.G., Foung, S.K., Liang, T.J., 2002. Structural features of envelope proteins on hepatitis C virus-like particles as determined by anti-envelope monoclonal antibodies and CD81 binding. Virology 298, 124–132.

von Heijne, G., 1988. Transcending the impenetrable: how proteins come to terms with membranes. Biochim. Biophys. Acta 947, 307–333.

Walter, A., Eidelman, O., Ollivon, M., Blumenthal, R., 1990. Functional reconstitution of viral envelopes. In: "Membrane Fusion" Wilschut, J., Hoekstra, D. (Eds.), Marcel Dekker, Inc., pp. 395–418.

World Health Organization, 1999. Global surveillance and control of hepatitis C. J. Viral Hepatitis 6, 35–47.

Wyatt, R., Moore, J.P., Accola, M., Desjardin, E., Robinson, J., Sodroski, J., 1995. Involvement of the V1/V2 variable loop structure in the exposure of human immunodeficiency virus type 1 gp120 epitopes induced by receptor binding. J. Virol. 69, 5723–5733.

Yagnik, A.T., Lahm, A., Meola, A., Roccasecca, R.M., Ercole, B.B., Nicosia, A., Tramontano, A., 2000. A model for the hepatitis C virus envelope glycoprotein E2. Proteins 40, 355–366.

Human VAP-B Is Involved in Hepatitis C Virus Replication through Interaction with NS5A and NS5B

Itsuki Hamamoto,[1] Yorihiro Nishimura,[1,2] Toru Okamoto,[1] Hideki Aizaki,[2,3] Minyi Liu,[3]
Yoshio Mori,[1] Takayuki Abe,[1] Tetsuro Suzuki,[2] Michael M. C. Lai,[3] Tatsuo Miyamura,[2]
Kohji Moriishi,[1] and Yoshiharu Matsuura[1]*

*Department of Molecular Virology, Research Institute for Microbial Diseases, Osaka University, Osaka,[1] and Department
of Virology II, National Institute of Infectious Diseases, Tokyo,[2] Japan, and Department of Molecular Microbiology and
Immunology, Keck School of Medicine, University of Southern California, Los Angeles, California[3]*

The hepatitis C virus (HCV) nonstructural protein (NS) 5A is a phosphoprotein that associates with various cellular proteins and participates in the replication of the HCV genome. Human vesicle-associated membrane protein-associated protein (VAP) subtype A (VAP-A) is known to be a host factor essential for HCV replication by binding to both NS5A and NS5B. To obtain more information on the NS5A protein in HCV replication, we screened human brain and liver libraries by a yeast two-hybrid system using NS5A as bait and identified VAP-B as an NS5A-binding protein. Immunoprecipitation and mutation analyses revealed that VAP-B binds to both NS5A and NS5B in mammalian cells and forms homo- and heterodimers with VAP-A. VAP-A interacts with VAP-B through the transmembrane domain. NS5A interacts with the coiled-coil domain of VAP-B via 70 residues in the N-terminal and 341 to 344 amino acids in the C-terminal polyproline cluster region. NS5A was colocalized with VAP-B in the endoplasmic reticulum and Golgi apparatus. The specific antibody to VAP-B suppressed HCV RNA replication in a cell-free assay. Overexpression of VAP-B, but not of a mutant lacking its transmembrane domain, enhanced the expression of NS5A and NS5B and the replication of HCV RNA in Huh-7 cells harboring a subgenomic replicon. In the HCV replicon cells, the knockdown of endogenous VAP-B by small interfering RNA decreased expression of NS5B, but not of NS5A. These results suggest that VAP-B, in addition to VAP-A, plays an important role in the replication of the HCV genome.

Hepatitis C virus (HCV) infects 170 million people worldwide and frequently leads to cirrhosis or hepatocellular carcinoma (6, 29). HCV is classified in the family *Flaviviridae* and possesses a single-stranded positive-sense RNA with a length of 9.6 kb. The HCV genome encodes a single large precursor polyprotein composed of about 3,000 amino acids (aa) that is processed by cellular and viral proteases, resulting in at least 10 structural and nonstructural (NS) proteins (29). Details of HCV's replication cycle are unknown because of the low viral load in the sera of HCV-infected individuals and the lack of a reliable and robust cell culture system to support HCV infection and replication. The development of HCV RNA replicons in which a synthetic HCV genomic or subgenomic RNA replicates efficiently in the human hepatocarcinoma cell line Huh-7 has enabled the study of viral RNA replication in cell culture (4, 20, 24). The HCV RNA replication complex, composed of the viral NS proteins and host cellular proteins, replicates the viral RNA genome at the intracellular membrane. Thus far, the HCV replicon system has greatly contributed to the understanding of HCV replication and pathogenesis associated with the expression of viral NS proteins. Replication of positive-strand RNA viruses generally involves certain intracellular membrane structures, including the endoplasmic reticulum (ER), Golgi apparatus, endosome, and lysosome (39).

Recently, several groups have succeeded in demonstrating cell-free replication activities of replication complexes in crude membrane fractions of HCV subgenomic replicon cells (2, 3, 14, 53). These cell-free systems provide semi-intact polymerase assays for biochemical dissection of HCV RNA replication and are a useful source for the isolation of HCV replication complexes. Replication complexes were detected in detergent-resistant membrane structures, most likely lipid raft structures (2, 14). Although HCV NS proteins presumably form a membrane-associated RNA replication complex with host proteins, the precise components and mechanisms for replication are poorly understood.

HCV NS5A is a phosphoprotein that appears to possess multiple and diverse functions in viral replication, interferon resistance, and pathogenesis (26, 35). Cell culture-adaptive mutations have been shown to cluster in the central portion of NS5A in subgenomic HCV replicons, indicating that NS5A is involved in the viral replication process either directly or by interacting with host cellular proteins (4, 55). This observation, together with the modulation of NS5A hyperphosphorylation by NS3, NS4A, and NS4B and physical interaction with other viral NS proteins, strongly supports the notion that NS5A is an essential component of the HCV replication complex (21, 30, 36). NS5A has been shown to be associated with a range of cellular proteins involved in cellular signaling pathways, such as interferon-induced kinase PKR (11), growth factor receptor-binding protein 2 (Grb2) (45), p53 (27, 37), phosphoinositide-3-kinase p85 subunit (15), and proteins in protein trafficking and membrane morphology, such as karyopherin β3 (8),

* Corresponding author. Mailing address: Department of Molecular Virology, Research Institute for Microbial Diseases, Osaka University, 3-1, Yamadaoka, Suita, Osaka 565-0871, Japan. Phone: 81-6-6879-8340. Fax: 81-6-6879-8269. E-mail: matsuura@biken.osaka-u.ac.jp.
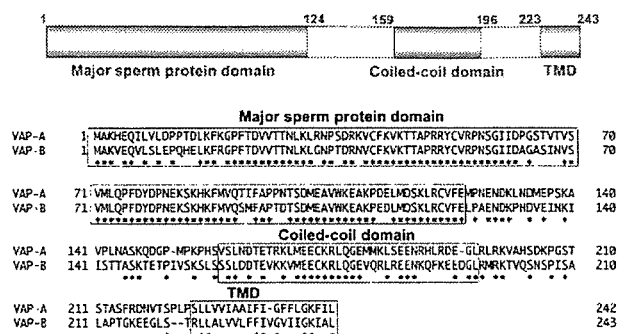
13473

FIG. 1. Schematic representation of VAP-B and alignment of amino acid sequences of VAP-A and VAP-B. The major sperm protein domain, coiled-coil domain, and TMD are indicated. The asterisks indicate identical amino acid residues between VAP-A and VAP-B.

apolipoprotein A1 (40), amphiphysin II (56), and vesicle-associated membrane protein (VAMP)-associated protein (VAP) subtype A (VAP-A), also called VAP-33 (48). Host fatty acids and geranylgeranylation appear to modulate the host and viral proteins involved in HCV RNA replication (19, 49, 54). Gao et al. showed that small interfering RNA (siRNA) or the dominant-negative mutant of VAP-A resulted in relocation of NS5B from detergent-resistant to detergent-sensitive membranes and reduced HCV RNA replication (12). In addition, Evans et al. suggested that NS5A hyperphosphorylation disrupts interaction with VAP-A and negatively regulates HCV RNA replication (9). Like many of the fusion proteins, VAP is a tail-anchored protein with a globular amino-terminal domain followed by a stalk region containing a coiled coil (Fig. 1), and it is ubiquitously expressed in human tissues (7). In humans, there are two isoforms of VAP, VAP-A and VAP-B, encoded by separate genes, and VAP-C is a splicing variant of VAP-B missing the C-terminal two-thirds (23, 32). VAP-B shows 63% amino acid identity to VAP-A (32, 51). The first proposed function for VAP arose from its initial identification as an interactor with the membrane fusion protein synaptobrevin/VAMP in *Aplysia* (43). Since then, it has been shown to be involved in vesicle transport, including the regulation of COP-I vesicle transport in the ER/Golgi pathway (13, 44), VAMP/synaptobrevin-mediated neurotransmitter release (38), and VAMP-2-mediated Glut-4 trafficking at the plasma membrane (10); it is also involved in the interaction between the microtubule network and tight junctions (22). Recently, VAP has been linked to the function of mammalian neurons, where VAP is enriched on microtubules (42), because a mutation in human VAP-B causes familial amyotrophic lateral sclerosis type 8 (32).

To gain a better understanding of the interactions between NS5A and host proteins involved in HCV replication, we screened human libraries by a yeast two-hybrid system using NS5A as bait and identified VAP-B as an NS5A-binding protein. In this study, we examined the biological significance of the interaction between VAP-B and NS proteins in HCV replication and found that VAP-B binds to both NS5A and NS5B in mammalian cells and forms homo- and heterodimers with VAP-A. Immunodepletion of VAP-B suppressed the replication of HCV RNA in a cell-free replication assay, and the

knockdown of endogenous VAP-B by siRNA decreased the expression of NS5B but not that of NS5A. These results suggest that VAP-B plays an important role in HCV replication through interaction with NS5A and NS5B.

MATERIALS AND METHODS

Cells. Human embryo kidney 293T, human cervical carcinoma HeLa, and human hepatoma Huh-7 cell lines were maintained in Dulbecco's modified Eagle's medium (DMEM) (Sigma, St. Louis, Mo) containing 10% fetal calf serum (FCS), while the Huh-9-13 cell line, which possesses an HCV subgenomic replicon (4, 20, 23), was cultured in DMEM supplemented with 10% FCS and 1 mg/ml G418. All cells were cultured at 37°C in a humidified atmosphere with 5% CO_2.

Antibodies. Chicken anti-human VAP-B antibody was prepared by immunization using the synthetic peptides of residues from 188 to 203. KQFKEEDGL RMRKTVQ, of human VAP-B. A mouse monoclonal antibody to human VAP-A was purchased from BD Pharmingen (San Diego, CA). Mouse monoclonal antibodies to giantin, influenza virus hemagglutinin (HA), and GluGlu (EE) tag were from Covance (Richmond, CA). Mouse anti-FLAG antibody M2, horseradish peroxidase-conjugated antibody, and mouse monoclonal anti-beta-actin antibody were from Sigma. A mouse monoclonal antibody to protein disulfide isomerase (PDI) was from Affinity Bioreagents (Golden, CO). Rabbit polyclonal antibody to NS5A was prepared by immunization using peptides of residues from 409 to 422. DVESYSSMPPLEGE. Mouse monoclonal antibody to NS5B was described previously (41).

Plasmids. For expression in mammalian cells, a DNA fragment encoding NS5A was generated from HCV genotype 1b strain J1 (1) (GenBank database accession number D89815), and another was generated from genotype 1a strain H77 (52) (GenBank database accession number AF009606) by PCR using *Pfu* turbo DNA polymerase (Stratagene, La Jolla, CA). The fragments were then cloned into the appropriate sites in pEF-FLAG pGBK puro (18) and pEGFP-C3 (Clontech, Palo Alto, CA). The mutations of the NS5A gene were generated by a method known as "splicing by overlapping extension" (16, 17) and cloned into pEF-FLAG pGBK puro. The DNA fragment encoding NS5B of the J1 strain was generated by PCR and cloned into pCAGGs-PUR (33). The DNA fragment encoding human VAP-A was amplified by PCR from a human fetal-brain library (Clontech) and was introduced into pEF-FLAG pGBK puro, pEF-EE hygro (34). pCHA3 (34), and pcDNA3.1-N-HA, in which an HA tag is inserted in the N terminus of the cloning site of pcDNA3.1(+) (Invitrogen, Carlsbad, CA). The cDNAs of human VAP-A and -B were amplified by PCR and cloned into pEF-FLAG pGBK puro, pEF-EE hygro, pcDNA3.1-N-HA, and pEGFP-C3. The genes encoding VAP lacking the transmembrane domain were amplified and cloned into pEF-FLAG pGBK puro. The DNA fragment encoding the human VAP-B protein lacking a coiled-coil region was introduced into pEF-EE hygro. All PCR products were confirmed by sequencing them with an ABI PRSM 310 genetic analyzer (Applied Biosystems, Tokyo, Japan).

Yeast two-hybrid assay and library screening. The NS5A-binding protein was identified by a yeast two-hybrid assay according to the user manual of MATCH-MAKER GAL4 Two-Hybrid System 3 (Clontech). The DNA fragment encoding amino acids 1973 to 2419 was amplified from HCV strain J1 by PCR and then was cloned into pGBKT7 (Clontech). The resulting plasmid was designated pGBK T7 HCV NS5A. A human brain library based on pACT2 was purchased from Clontech. The yeast *Saccharomyces cerevisiae* strain AH109, which secretes alpha-galactosidase under the control of MEL1 upstream activation sequence, was grown in yeast extract-peptone-dextrose medium and transformed with the bait and library plasmids. The transformed yeast cells were grown on 2.0% agar plates of dropout medium lacking tryptophan, leucine, histidine, and adenine. The resulting colonies were inoculated on the new dropout plate containing 20 μg/ml X-alpha-Gal (5-bromo-4-chloro-3-indolyl-alpha-O-galactopyranoside) and lacking leucine and tryptophan. The total DNA was prepared from all positive clones and then introduced into *Escherichia coli* strain JM109. The prey plasmids of isolated yeast cells were recovered from the clones grown on LB agar plates containing 10 μg/ml ampicillin and then purified. The insert DNA fragments of isolated clones were determined by sequencing. Finally, 48 alpha-galactosidase-positive clones were identified from 2 million clones screened in the fetal-brain library. One of the positive clones contained the complete cDNA of human VAP-B in frame.

Transfection, immunoblotting, and immunoprecipitation. Cells were seeded onto a six-well tissue culture plate 24 h before transfection. The plasmids were transfected into cells by liposome-mediated transfection using Lipofectamine 2000 (Invitrogen). Cells were harvested 36 h posttransfection, washed five times

with 1 ml of ice-cold phosphate-buffered saline (PBS), and suspended in 0.2 ml lysis buffer (20 mM Tris-HCl, pH 7.4, containing 135 mM NaCl and 1% Triton X-100) supplemented with 1 μg/ml leupeptin, 50 mM NaF, 1 mM phenylmethylsulfonyl fluoride, and 5 mM NaVO₄. Cell lysates were sonicated at 4°C for 5 min, incubated for 30 min at 4°C, and centrifuged at 14,000 × g for 5 min at 4°C. The supernatant was immunoprecipitated with 1 μg of antibodies and 10 μl of Protein G-Sepharose 4B Fast Flow beads (Amersham Pharmacia Biotech, Franklin Lakes, NJ). The immunocomplex was precipitated with the beads by centrifugation at 14,000 × g for 30 s and then was washed five times with lysis buffer by centrifugation. The proteins binding to the beads were boiled in 30 μl of loading buffer and then subjected to sodium dodecyl sulfate-12.5% polyacrylamide gel electrophoresis. The proteins were transferred to polyvinylidene difluoride membranes (Millipore, Bedford, MA) and then reacted with primary antibody and secondary horseradish peroxidase-conjugated antibody. The immunocomplexes were visualized with Super Signal West Femto substrate (Pierce, Rockford, IL) and detected by using an LAS-3000 image analyzer (Fujifilm, Tokyo, Japan).

Immunofluorescence microscopy. Cells were seeded on an eight-well chamber slide at 2 × 10⁴ per well 24 h before transfection. Transfected cells were washed twice with PBS, fixed with PBS containing 4% paraformaldehyde, and permeabilized with PBS containing 0.5% Triton X-100. The ER and Golgi apparatus of cells were stained with the mouse monoclonal antibody against luminal ER redox enzyme PDI and the rabbit polyclonal antibody against giantin, respectively, in PBS containing 5% bovine serum albumin. Bound primary antibody was revealed with Alexa Fluor 594-conjugated anti-mouse or anti-rabbit antibody. After additional washes with PBS, a coverslip was attached over PBS containing 50% glycerol and observed under an LSM 510 microscope (Carl Zeiss, Tokyo, Japan).

Gene silencing by siRNA. The siRNA target sequence against human VAP-B, 5′-GGUUAUGGAAGAAUGUAAGUU-3′, was synthesized and purified by Ambion (Austin, TX). Negative control siRNA, siCONTROL Non-Targeting siRNA-2, was purchased from Dharmacon (Lafayette, CO). The Huh-7 cells harboring a subgenomic HCV replicon on six-well plates were transfected with 80 nM or 160 nM of siRNA by using siFECTOR (B-Bridge International, Sunnyvale, CA) according to the manufacturer's protocol. Cells were incubated in DMEM supplemented with 10% FCS and harvested at 96 h posttransfection.

RNA replication assay. In vitro RNA replication was determined as previously described with some modification (3). Briefly, the Huh-7 cells harboring a subgenomic HCV replicon grown in a 100-mm dish were treated with lysolecithin (Wako, Osaka, Japan) (250 μg/ml in wash buffer: 150 mM sucrose, 30 mM HEPES [pH 7.4], 33 mM NH₄Cl, 7 mM KCl, 4.5 mM magnesium acetate), collected by scraping in 120 μl of incomplete replication buffer (100 mM HEPES [pH 7.4], 50 mM NH₄Cl, 7 mM KCl, and 1 mM spermidine), and centrifuged at 1,600 rpm for 5 min at 4°C. A total of 40 μl of cytoplasmic fraction (supernatant) was treated with 1% Nonidet P-40 (Boehringer Mannheim, Quebec, Canada) at 4°C for 1 h and incubated with antibody for 4 h at 4°C with rotation. Then, samples were incubated with 1 mM of ATP, GTP, and UTP; 10 μM CTP; [α-³²P]CTP (1 MBq; 15 TBq/mmol); 10 μg/ml actinomycin D; and 800 U/ml RNase inhibitor (Promega, Madison, WI) for 4 h at 30°C. RNA was extracted from the total mixture by TRI Reagent (Molecular Research Center Inc., Cincinnati, OH). The RNA was precipitated, eluted in 10 μl of RNase-free water, and analyzed by 1% formaldehyde agarose gel electrophoresis.

Real-time PCR. Total RNA was prepared from cell lines by using TRIzol LS (Invitrogen), and first-strand cDNA was synthesized by using a first-strand cDNA synthesis kit (Amersham) with random primers. Each cDNA was estimated by Platinum SYBR Green qPCR SuperMix UDG (Invitrogen) according to the manufacturer's protocol. Fluorescent signals were analyzed with an ABI PRISM 7000 (Applied Biosystems). The HCV NS5A gene was amplified using the primer pairs 5′-AGTCAGTTGTCTGCGCTTTC-3′ and 5′-CGGGGAATTTCCTGGT CTTC-3′. The human beta-actin gene was amplified with the primer pairs 5′-T GGAGTCCTGTGGCATCCACGAAACTACCTTCAACTC-3′ and 5′-CGGA CTCGTCATACTCCTGCTTGCTGATCCACATC-3′, which are located at different exons to prevent false-positive amplification from contaminated genomic DNA. The value of the HCV genome was normalized with that of actin mRNA. Each PCR product was found as a single band of the correct size on agarose gel electrophoresis (data not shown).

RESULTS

Isolation of VAP-B as a novel binding partner for HCV NS5A. To examine the protein(s) that interacts with NS5A in more detail, we screened a cDNA library of human fetal brain by a yeast two-hybrid system using a full-length NS5A of ge-
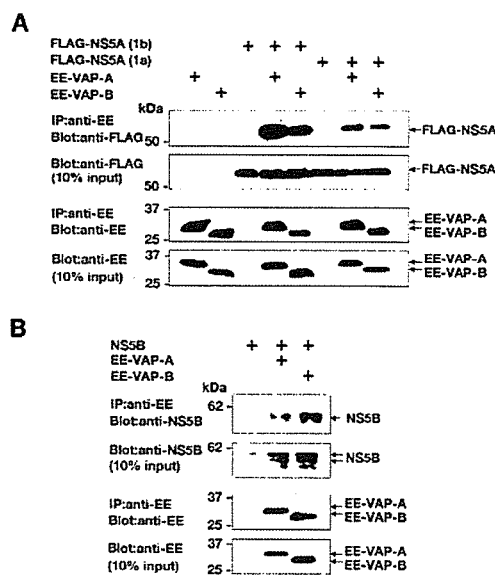

FIG. 2. VAP-A and VAP-B bind to both NS5A and NS5B in mammalian cells. N-terminally FLAG-tagged NS5A of genotype 1b, FLAG-NS5A (1b) of genotype 1a, FLAG-NS5A (1a), and N-terminally EE-tagged VAP (EE–VAP-A or EE–VAP-B) were coexpressed in HEK293T cells and immunoprecipitated with anti-EE antibody. The resulting precipitates were examined by immunoblotting using anti-FLAG antibody (A). NS5B was coexpressed with EE-tagged VAP-A or VAP-B and immunoprecipitated with anti-EE antibody, and NS5B in the precipitates was detected by anti-NS5B antibody (B). One-tenth of the lysates used in immunoprecipitation are shown as the 10% input. The data in each panel are representative of three independent experiments.

notype 1b as bait. Among the 2 million transformants we screened, we obtained 48 positive clones containing cDNAs that encode proteins interactive with NS5A. A BLAST search against the GenBank database revealed each of two clones that have the cDNA encoding VAP-A and VAP-B in frame. Figure 1 shows the amino acid alignments of VAP-A and VAP-B and their predicted functional domains. VAP-A and VAP-B are composed of 242 and 243 amino acids, respectively. VAP-B shows 63% amino acid identity to VAP-A. VAP has three structural domains. The first 124 amino acids share high sequence similarity with the nematode major sperm protein and are conserved among all VAP family members (50). The central region on the protein contains an amphipathic helical structure and is predicted to form a coiled-coil protein-protein interaction motif (159 to 196 aa) and a hydrophobic carboxy-terminal transmembrane domain (TMD) (223 to 243 aa). The homology between their N-terminal regions is higher than that between their C-terminal regions (32, 48).

VAP-B interacts with NS5A and NS5B in mammalian cells. To confirm the specific interaction, FLAG-tagged NS5A was coexpressed with EE-tagged VAP-A or VAP-B in 293T cells, and cell lysates were immunoprecipitated by specific antibodies. NS5A was coprecipitated with VAP-A and VAP-B to similar extents (Fig. 2A). We also obtained the same results in the reverse experiments (data not shown). Recently, it was shown that hyperphosphorylation of NS5A disrupts interaction with VAP-A and negatively regulates HCV RNA replication, sug-

gesting that adaptive mutations detected in the HCV replicon prevent phosphorylation-dependent dissociation of the RNA replication complex (9). Amino acid residues at Tyr2185 and Lys2187 of NS5A genotype 1b were defined as key determinants for VAP-A binding, and the replacement of these residues with those of genotype 1a (Ala and Gly, respectively) reduced binding to VAP-A in yeast and enhanced hyperphosphorylation of NS5A (9). However, as shown in Fig. 2A, the NS5As of both the 1a and 1b genotypes were coimmunoprecipitated with VAP-A and -B in mammalian cells. Since a previous report indicated that VAP-A interacts with not only NS5A but also NS5B (12), we next examined the interaction of VAP-B with NS5B. EE-tagged VAP-A or VAP-B was coexpressed with NS5B in 293T cells and immunoprecipitated with anti-EE-tag antibody. NS5B was coprecipitated with VAP-B, as well as VAP-A (Fig. 2B). These results indicate that VAP-B participates in the complex of HCV NS proteins in a manner similar to that of VAP-A.

NS5A colocalizes with VAP-B in ER and Golgi compartments. To determine the subcellular localization of NS5A and VAP-B in mammalian cells, HeLa cells were cotransfected with plasmids encoding enhanced green fluorescent protein (EGFP)-tagged NS5A and FLAG-tagged VAP-B or FLAG-tagged VAP-A and examined by immunofluorescence analysis. EGFP-NS5A was colocalized exclusively with FLAG-VAP-B in the cytoplasm, as seen in FLAG-VAP-A (Fig. 3A). To further determine the precise subcellular localization of NS5A and VAP-B, the ER and Golgi apparatus were stained with specific antibodies against PDI and giantin, respectively. NS5A and VAP-B were colocalized with PDI and giantin in HeLa cells transfected with the plasmids (Fig. 3B), indicating that NS5A and VAP-B are colocalized in the membranes of the ER or ER-derived compartment. VAP-B was localized in a diffuse ER-like network, in small vesicles clustered around the nucleus, and predominantly in a perinuclear/Golgi region. Similar to the case with VAP-A, the colocalization of NS5A with VAP-B in the ER and Golgi apparatus suggests that NS5A specifically interacts with VAP-B under intracellular conditions.

Dimerization of VAP-A and VAP-B and interaction with NS5A. Immunoprecipitation analyses revealed that NS5A and NS5B interact with VAP-A and VAP-B. Therefore, it might be reasonable to speculate that VAP-A and VAP-B interact with each other and are involved in RNA replication through the formation of a replication complex. It has been demonstrated that VAP-A interacts with VAP-A or VAP-B through their TMDs and forms a homodimer and a heterodimer in vitro (32). We constructed expression plasmids encoding mutant VAP-A and VAP-B lacking their TMDs and examined their dimer formation with authentic VAPs in vivo. Although coprecipitation of authentic VAP (FLAG–VAP-B or FLAG–VAP-A) with VAP-B–HA was clearly detected, no interaction between TMD deletion mutants (FLAG–VAP-AΔTMD or FLAG–VAP-BΔTMD) and VAP-B–HA was observed (Fig. 4A and B). Furthermore, a TMD deletion mutant, HA–VAP-BΔTMD, which lost the ability to form a dimer with VAP-B and VAP-A, retained the ability to bind to FLAG-NS5A (Fig. 4C), although the efficiency of interaction with NS5A was reduced. These results indicate that TMDs of VAP-A and VAP-B are required for hetero- and homodimerization, but
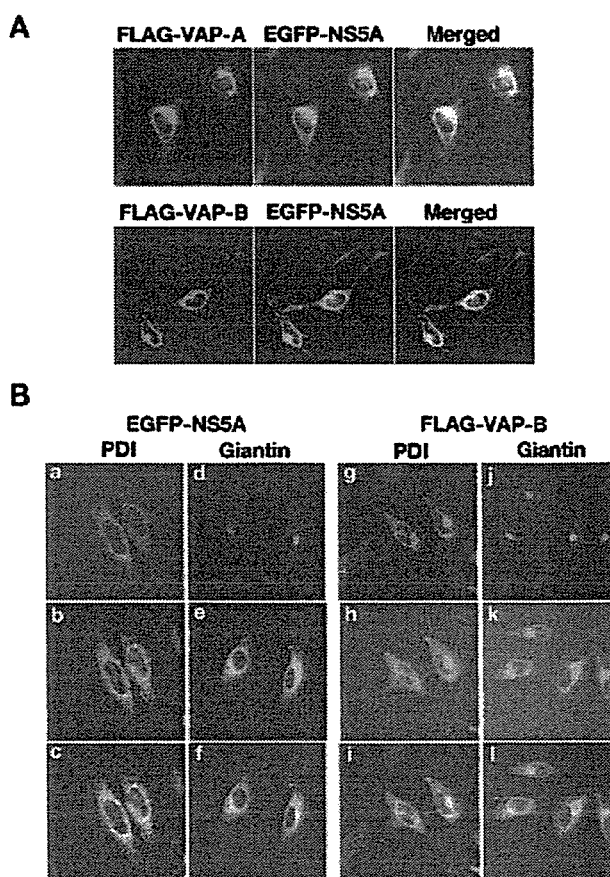

FIG. 3. Intracellular localization of VAPs and NS5A in mammalian cells. (A) N-terminally FLAG-tagged VAP (FLAG–VAP-A or FLAG–VAP-B) was coexpressed with N-terminally EGFP-fused NS5A of genotype 1b (EGFP-NS5A) in HeLa cells, fixed with 4% paraformaldehyde-PBS, permeabilized with 0.5% Triton X-100, and stained with anti-FLAG antibody and AlexaFluor 594-conjugated anti-mouse IgG antibody. (B) EGFP-NS5A of genotype 1b (b and e) or FLAG–VAP-B (h and k) was expressed and then stained with anti-PDI (a and g) or anti-giantin (d and j) antibodies and AlexaFluor 594-conjugated anti-mouse IgG antibody. FLAG–VAP-B was stained with biotinylated anti-FLAG antibody and fluorescein isothiocyanate-conjugated streptavidin. Overlapped images are shown in panels c, f, i, and l.

not for binding to NS5A. A region other than the TMD should be involved in the specific interaction between VAP-B and HCV NS5A. The coiled-coil domain of VAP-A was reported to be critical for binding to NS5A (48). Therefore, we examined whether the coiled-coil domain of VAP-B is also involved in interaction with NS5A. FLAG-NS5A was coimmunoprecipitated with EE–VAP-B but not with EE–VAP-BΔcoiled-coil, which lost the coiled-coil domain but retained the TMD (Fig. 4D), suggesting that the coiled-coil domain is also essential for interaction between NS5A and VAP-B.

Two separate domains in NS5A are critical for binding to VAP-B. Since NS5A specifically interacts with VAP-B, we tried to determine the region of NS5A responsible for interaction with VAP-B. Various deletion mutants of FLAG-tagged NS5A were prepared as shown in Fig. 5A. The mutants covering regions from amino acids 1 to 75, but not 1 to 50, and those